

# Multi-layer Cross-Attention is Provably Optimal for Multi-modal In-context Learning

Nicholas Barnfield<sup>1</sup>, Subhabrata Sen<sup>1</sup>, and Pragya Sur<sup>1</sup>

<sup>1</sup>Department of Statistics, Harvard University

April 29, 2026

## Abstract

Recent progress has rapidly advanced our understanding of the mechanisms underlying in-context learning in modern attention-based neural networks. However, existing results focus exclusively on unimodal data; in contrast, the theoretical underpinnings of in-context learning for multi-modal data remain poorly understood. We introduce a mathematically tractable framework for studying multi-modal learning and explore when transformer-like architectures can recover Bayes-optimal performance in-context. To model multi-modal problems, we assume the observed data arises from a latent factor model. Our first result comprises a negative take on expressibility: we prove that single-layer, linear self-attention fails to recover the Bayes-optimal predictor uniformly over the task distribution. To address this limitation, we introduce a novel, linearized cross-attention mechanism, which we study in the regime where both the number of cross-attention layers and the context length are large. We show that this cross-attention mechanism is provably Bayes optimal when optimized using gradient flow. Our results underscore the benefits of depth for in-context learning and establish the provable utility of cross-attention for multi-modal distributions.

## 1 Introduction

Large language models exhibit striking “in-context learning” (ICL) behavior [Brown et al., 2020]: given a sequence of input-output pairs for a new task, the model can infer the rule (the function from input to output) without any update to the model weights. This phenomenon has motivated a growing body of theoretical work that tries to understand when and how ICL succeeds in linearized attention-based models [Zhang et al., 2024a, Lu et al., 2025, Zhang et al., 2025].

Prior work on ICL focuses on unimodal data; in contrast, modern foundation models routinely process multi-modal data, such as text, images, video [Li et al., 2024], multi-omic data [Cui et al., 2025], etc. This prompts the natural question:

*Can attention-based neural networks learn prediction rules in-context when deployed on multi-modal datasets?*

In this work, we formulate and study an ICL problem on multi-modal data. Our main contributions are as follows:

- We introduce a statistical model for ICL on multi-modal data. The proposed data distribution is a latent factor model where the factors are dependent across the data modalities.

- We show that a single-layer, linear self-attention (LSA) model fails to achieve Bayes-optimal performance in-context over this class of data distributions.
- We propose a multi-layer model with cross-attention (CA) plus self-attention (SA) and skip connections to solve the ICL problem in this context. Linearizing the attention mechanism, we show that, upon a suitable restriction of the model parameters, gradient flow on the population loss converges to the Bayes-optimal ICL predictor.

To highlight the technical challenge in our setting, note that prior work on ICL in a regression setting assumes that the covariates are sampled from a fixed distribution (usually Gaussian) independent of the learning task [Zhang et al., 2024a, 2025, Lu et al., 2025]. Indeed, [Zhang et al., 2024a, 2025] explicitly notes that the invariance of the covariate distribution across prompts is crucial in establishing the success of single-layer LSA. In sharp contrast, our multi-modal model exhibits covariate-shifts across prompts. In addition, the prediction rule in a prompt is naturally coupled with the covariate distribution in our setting. In Theorem 4.1, we formally establish that the natural covariate shift in our setup invalidates single-layer LSA (i.e., models based on single-layer LSA fail to be Bayes optimal). To overcome this challenge, we introduce a multi-layer model based on both linear cross-attention (LCA) and LSA, and show that it succeeds on the ICL task.

At an intuitive level, the success of attention-based neural networks is derived from their ability to learn “long-range” relations among the features. In multi-modal learning, it is critical to learn the dependence among features across the observed modalities. The CA mechanism has been suggested as a natural extension of the attention mechanism to this end [Vaswani et al., 2017, Lu et al., 2019]; in our work, we demonstrate the efficacy of deep neural networks which use both LCA and LSA layers for multi-modal learning.

**Paper organization.** The rest of the paper is organized as follows. In Section 2, we review prior work on ICL and multi-modal learning. In Section 3, we introduce the latent-factor data distribution. In Section 4, we define the ICL objective and show a single-layer LSA baseline fails at the ICL task. In Sections 5–6, we propose the multi-layer CA architecture and show that gradient flow converges to the Bayes-optimal in-context prediction. In Section 7, we present supporting numerical experiments, and then conclude in Section 8 with discussion and future directions. Full proofs are left for Appendices A–E. Appendices F–G include additional numerics.

## 2 Prior Work

ICL capabilities of large language models were first noted in [Brown et al., 2020]. These observations motivated significant recent research on the foundations and intricacies of ICL. Early investigations focused on the expressivity of transformers [Bai et al., 2023, Akyürek et al., 2023, Garg et al., 2022] and demonstrated that their ICL capabilities enable them to implement common statistical algorithms and learn certain function classes. Connections of ICL with meta-learning and variants of gradient descent were noted in [Von Oswald et al., 2023, Ahn et al., 2023, Zhang et al., 2024b]. Generalization and stability properties of ICL were studied in [Li et al., 2023], while a Bayesian interpretation was offered in [Xie et al., 2022].

Training dynamics of attention-based models and ICL performance of the trained models have also been investigated thoroughly. Perhaps the closest to our work is [Zhang et al., 2024a], which studies ICL in the context of regression, demonstrating that a single-layer LSA model trained by gradient flow on the population loss learns the Bayes-optimal predictor. Subsequently, gradient flow or descent dynamics for multi-head self-attention were studied in [Chen et al., 2024, Zhang et al., 2025]. The recent work [Huang et al., 2023] goes

beyond linearized attention models, and studies gradient descent on stylized one-layer transformers with non-linear softmax attention.

More recently, ICL has been studied for a wider variety of models ranging from Gaussian mixture classification and clustering to non-parametric regression [Shen et al., 2025, Maulen-Soto et al., 2025, Ma et al., 2025, Ching et al., 2026]. Attention-based models have also been studied through a Gaussian sequence multi-index modeling lens in [Cui et al., 2024, Arnaboldi et al., 2025, Troiani et al., 2025] and on sparse-token classification tasks [Oymak et al., 2023, Barnfield et al., 2025], although ICL was not necessarily a key focus in these lines of work.

In a different direction, ICL performance for infinite token dimension was studied in [Lu et al., 2025]; they uncovered interesting trade-offs for ICL with regards to the number of pretraining examples, task diversity and other problem parameters; see also [Wu et al., 2024] for the impact of the number of independent pretraining tasks. The recent work [Letey et al., 2025] investigated the impacts of pre-training and testing task covariance mismatch. Despite this extensive literature, these prior works are restricted to data arising from a single mode, whereas we focus on ICL for multi-modal data.

In diverse artificial intelligence problems, multi-modal learning—combining information from varied modes, e.g., text, image, video—is known to improve prediction, reasoning and learning capabilities. Although examined extensively in empirical studies [Radford et al., 2021, Alayrac et al., 2022, Jaegle et al., 2021, Wang et al., 2024], this setting is far from understood from a rigorous standpoint. Bridging this theoretical gap is a primary aim of our manuscript.

Specifically, multi-modal learning is useful when the modes share common information. To capture this, we use latent variable models that have been widely used in statistical estimation for studying multi-modal data. Relevant works in this regard include [Nandy and Ma, 2024, Ding et al., 2022, Mergny and Zdeborová, 2025, Keup and Zdeborová, 2025, Deshpande et al., 2018, Yang et al., 2025, Sergazinov et al., 2025]. However, these papers do not study ICL or attention-based models in this context. On the theoretical end, [Liu et al., 2025, Gui et al., 2025, Cai et al., 2024] study multi-modal contrastive learning, but do not focus on ICL, which is the main focus of our present work.

### 3 Problem Setup

**Notation.** Bold lower and upper case letters are used for vectors and matrices respectively. We use  $\mathbf{0}_{d \times d}$  and  $\mathbf{0}_d$  for the matrix and vector of all zero entries. We use  $\mathbf{I}_d$  to denote the identity matrix in  $\mathbb{R}^d$ , omitting the subscript at times when the ambient dimension is evident. The standard basis vectors are written as  $\mathbf{e}_j$  for  $j \geq 1$  to denote the vector of zeros except for a one in the  $j$ -th entry with the context implying the dimension. The multivariate Gaussian distribution in  $\mathbb{R}^d$  is written  $\mathcal{N}_d(\boldsymbol{\mu}, \boldsymbol{\Sigma})$  where  $\boldsymbol{\mu} \in \mathbb{R}^d$  denotes the mean and  $\boldsymbol{\Sigma} \in \mathbb{R}^{d \times d}$  denotes the covariance. Lastly, for  $k \in \mathbb{N}$ , we write  $[k] = \{1, 2, \dots, k\}$ .

We study a multi-modal framework where each prompt (task) provides a context of input–output examples; the inputs contain features from two distinct modalities. To model a natural multi-modal setting, we assume the data is drawn from a latent variable model. Unlike prior work on ICL, we allow the distribution of covariates to differ across tasks.

Formally, we observe  $N$  prompts (tasks) with (training) context length  $L$ . For each prompt  $j \in [N]$ , we observe a sequence

$$(\bar{\mathbf{z}}_i^{(j)}, \tilde{\mathbf{z}}_i^{(j)}, y_i^{(j)})_{i=1}^L$$

where  $y_i^{(j)} \in \mathbb{R}$  is a response and  $\bar{\mathbf{z}}_i^{(j)} \in \mathbb{R}^{d_1}, \tilde{\mathbf{z}}_i^{(j)} \in \mathbb{R}^{d_2}$  are two modalities of covariates. For example,  $\bar{\mathbf{z}}$  could represent an image,  $\tilde{\mathbf{z}}$  some associated text annotation, and  $y$  represents a real-valued output. In

each prompt, we additionally observe a tuple  $(\bar{z}_q^{(j)}, \tilde{z}_q^{(j)}, y_q^{(j)})$ . We input the prompt and the covariate pair  $(\bar{z}_q^{(j)}, \tilde{z}_q^{(j)})$  into the model, and it outputs a prediction  $\hat{y}_q^{(j)}$  for  $y_q^{(j)}$ . While training, the model weights are tuned to minimize the error in predicting the  $y_q$ 's on the training prompts. To assess the ICL performance of the fitted model, we consider a fresh prompt, and study the prediction error of the fitted model on the  $y_q$  associated with the test prompt.

We now turn to a statistical model for the data. The covariates and response are generated via

$$\begin{aligned}\bar{z}_i^{(j)} &= u_i^{(j)} \mathbf{v}^{(j)} + \boldsymbol{\xi}_i^{(j)} \\ \tilde{z}_i^{(j)} &= u_i^{(j)} \mathbf{r}^{(j)} + \boldsymbol{\eta}_i^{(j)} \\ y_i^{(j)} &= \zeta^{(j)} u_i^{(j)}.\end{aligned}\tag{3.1}$$

The latent variable  $u_i^{(j)} \stackrel{\text{i.i.d.}}{\sim} \mathcal{N}(0, 1)$  is shared across both modalities and the response. The prompt-specific regression coefficient, which relates  $u_i^{(j)}$  to  $y_i^{(j)}$ , is given by  $\zeta^{(j)} \in \mathbb{R}$ . We will assume that across prompts,  $\zeta^{(j)}$  are sampled i.i.d. from a distribution with mean 0 and variance 1. On the other hand,  $\mathbf{v}^{(j)} \in \mathbb{R}^{d_1}$  and  $\mathbf{r}^{(j)} \in \mathbb{R}^{d_2}$  are modality-specific vectors sampled i.i.d. across prompts. We defer precise assumptions about their distributions to later sections. Finally,  $\boldsymbol{\xi}_i^{(j)} \stackrel{\text{i.i.d.}}{\sim} \mathcal{N}_{d_1}(0, \mathbf{I})$  and  $\boldsymbol{\eta}_i^{(j)} \stackrel{\text{i.i.d.}}{\sim} \mathcal{N}_{d_2}(0, \mathbf{I})$  are i.i.d. noise variables, and all unique variables on the right-hand side of (3.1) are mutually independent. The setup in (3.1) formalizes mathematically a fundamental idea underlying multi-modal machine learning: each modality provides a different (noisy) view of a common latent feature  $u$  which drives the response  $y$ .

Focusing on a single task, omitting the prompt superscript, stacking the covariates and their modality vectors, we denote

$$\mathbf{x}_i := \begin{bmatrix} \bar{z}_i \\ \tilde{z}_i \end{bmatrix}, \quad \mathbf{m} := \begin{bmatrix} \mathbf{v} \\ \mathbf{r} \end{bmatrix}\tag{3.2}$$

and let  $d = d_1 + d_2$ . Then, in each prompt (i.e. conditional on  $\mathbf{m}$  and  $\zeta$ ), the covariates and response are jointly Gaussian

$$\begin{bmatrix} \mathbf{x}_i \\ y_i \end{bmatrix} \stackrel{\text{i.i.d.}}{\sim} \mathcal{N}_{d+1}(0, \boldsymbol{\Sigma}) \quad \text{with} \quad \boldsymbol{\Sigma} = \begin{bmatrix} \mathbf{I} + \mathbf{m}\mathbf{m}^\top & \zeta \mathbf{m} \\ \zeta \mathbf{m}^\top & \zeta^2 \end{bmatrix}.$$

The joint Gaussianity of the covariates and response allows us to write

$$y_i = \langle \mathbf{w}, \mathbf{x}_i \rangle + \varepsilon_i \quad \text{where} \quad \mathbf{w} = \frac{\zeta}{1 + \|\mathbf{m}\|^2} \mathbf{m}\tag{3.3}$$

$$\text{and} \quad \varepsilon_i \stackrel{\text{i.i.d.}}{\sim} \mathcal{N}(0, \zeta^2 / (1 + \|\mathbf{m}\|^2)).$$

Our goal is to learn the task-specific Bayes-optimal predictor  $\langle \mathbf{w}, \mathbf{x} \rangle$ . The setup (3.3) is reminiscent of the regression setting considered in prior work [Zhang et al., 2024a, Lu et al., 2025, Zhang et al., 2025], yet presents several differences that make the learning problem significantly more difficult. Upon setting

$$\boldsymbol{\Lambda} = \mathbf{I} + \mathbf{m}\mathbf{m}^\top\tag{3.4}$$

as the covariance of the covariates  $\{\mathbf{x}_i\}_{i=1}^L \cup \{\mathbf{x}_q\}$ , we note that the distribution of covariates varies across prompts, since  $\mathbf{m}$  is sampled anew for each task. Furthermore, the task vector  $\mathbf{w}$  and covariate distribution are coupled through  $\mathbf{m}$ . Similarly, the variance of the additive noise and the task vector are coupled through the task-specific parameter  $\zeta$ . These dependencies invalidate prior ICL theory in our setup.

As we will see below, this leads to the failure of single-layer linearized attention models previously shown to be successful for ICL when the covariate distribution does not change across prompts [Zhang et al., 2024a, 2025].

## 4 ICL and Failure of LSA

In this section, we introduce ICL formally and show that a single-layer LSA model fails at the ICL task. To this end, we represent a single prompt by its covariate matrix and target vector

$$\begin{aligned}\mathbf{X} &:= [\mathbf{x}_1, \dots, \mathbf{x}_L] \in \mathbb{R}^{d \times L}, \\ \mathbf{y} &:= [y_1, \dots, y_L]^\top \in \mathbb{R}^L,\end{aligned}$$

where we append a dummy zero label at the query position. We define the (non-learned) joint embedding matrix

$$\mathbf{E}_X := \begin{bmatrix} \mathbf{X} & \mathbf{x}_q \\ \mathbf{y}^\top & 0 \end{bmatrix} = \begin{bmatrix} \mathbf{x}_1 & \mathbf{x}_2 & \cdots & \mathbf{x}_L & \mathbf{x}_q \\ y_1 & y_2 & \cdots & y_L & 0 \end{bmatrix} \in \mathbb{R}^{(d+1) \times (L+1)}$$

which has been employed in recent works [Ahn et al., 2023, Zhang et al., 2024a, Chen et al., 2024, Huang et al., 2023]. A model  $f$  maps  $\mathbf{E}_X$  to a scalar prediction  $\hat{y}_q = f(\mathbf{E}_X)$  with the goal of approximating  $\hat{y}_q \approx y_q$ .

So far, the context length  $L$  is a free variable. In the subsequent discussion, it will be helpful to assume that the context length  $L = L_{\text{tr}}$  for prompts in the training data. We set  $L = L_{\text{te}}$  to denote the context length at test time. Our model architecture is independent of the context length, and thus this distinction is mostly for mathematical convenience. The parameter  $L_{\text{te}}$  governs the generalization performance of the fitted model.

### 4.1 ICL Definition

**Formal ICL Criterion.** Let  $\hat{y}_q^{(L_{\text{te}})}$  denote the model prediction on a new prompt when the test context length  $L = L_{\text{te}}$ . We say a model *in-context learns* if

$$\hat{y}_q^{(L_{\text{te}})} \longrightarrow y_q^{\text{Bayes}} := \mathbb{E}[y_q | \mathbf{m}, \zeta, \mathbf{x}_q] = \langle \mathbf{w}, \mathbf{x}_q \rangle \quad (4.1)$$

almost surely as  $L_{\text{te}} \rightarrow \infty$ , where the almost sure statement is with respect to the randomness of the new prompt. In words, ICL in our framework is synonymous with the model recovering the *Bayes-optimal predictor*  $y_q^{\text{Bayes}}$  almost surely in the asymptotic  $L_{\text{te}} \rightarrow \infty$  limit.

The criterion (4.1) matches the mathematical interpretation of ICL in prior work [Zhang et al., 2024a], although unlike in the linear regression setup [Garg et al., 2022, Zhang et al., 2024a, Lu et al., 2025], the task vector  $w$ , the covariate distribution and the variance of the errors are all coupled via the latent variables  $\mathbf{m}$ ,  $\zeta$ .

### 4.2 Baseline Model

As a starting point, we study a simple baseline model and show its inability to in-context learn in our setting.

**Single-layer LSA.** We consider a single LSA layer acting on  $\mathbf{E}_X$  as seen in a line of prior works [Von Oswald et al., 2023, Ahn et al., 2023, Zhang et al., 2024a, Lu et al., 2025]. We write  $\text{LSA}(\mathbf{E}_X; \theta) \in \mathbb{R}^{(d+1) \times (L+1)}$ ,

$$\text{LSA}(\mathbf{E}_X; \theta) = \mathbf{E}_X + \mathbf{W}^{PV} \mathbf{E}_X \cdot \frac{\mathbf{E}_X^\top \mathbf{W}^{KQ} \mathbf{E}_X}{L} \quad (4.2)$$

where  $\theta = \{\mathbf{W}^{PV}, \mathbf{W}^{KQ}\}$  are learnable weight matrices and the model’s prediction is taken to be  $\hat{y}_q = (\text{LSA}(\mathbf{E}_X; \theta))_{d+1, L+1}$ . This model is a linearized analogue of a transformer block

$$\begin{aligned} & \text{SA}(\mathbf{E}_X; \theta) \\ &= \mathbf{E}_X + \mathbf{W}^P \mathbf{W}^V \mathbf{E}_X \cdot \text{softmax} \left( \frac{(\mathbf{W}^K \mathbf{E}_X)^\top \mathbf{W}^Q \mathbf{E}_X}{L} \right), \\ & \theta = \{\mathbf{W}^P, \mathbf{W}^V, \mathbf{W}^K, \mathbf{W}^Q\}, \end{aligned} \tag{4.3}$$

without nonlinearities and normalization, and with tied parameters  $\mathbf{W}^{KQ} = (\mathbf{W}^K)^\top \mathbf{W}^Q$  and  $\mathbf{W}^{PV} = \mathbf{W}^P \mathbf{W}^V$ . Collapsing the key and query, and the projection and value weight matrices into single matrices for the LSA model differs from a practical transformer implementation, but is mathematically identical in regards to expressibility.

In demonstrating the success of the LSA model in unimodal ICL tasks, prior works [Zhang et al., 2024a] rely on proving that the parameters  $\theta$  can emulate a global, inverse, covariance  $\mathbf{\Lambda}^{-1}$ . However, in the multi-modal setting, as the covariance  $\mathbf{\Lambda}$  is random, no fixed parameters  $\theta$  can perform this role and hence the LSA model fails at the ICL task as shown in Theorem 4.1.

**Theorem 4.1** (Single-layer LSA fails at ICL). *In the setting of Section 3, and assuming  $\|\mathbf{m}\|$  and  $\zeta$  are atomless <sup>1</sup>, no single-layer LSA predictor  $\hat{y}_q = (\text{LSA}(\mathbf{E}_X; \theta))_{d+1, L_{\text{te}}+1}$  can in-context learn in the sense of (4.1). In particular, for any fixed  $\theta = \{\mathbf{W}^{PV}, \mathbf{W}^{KQ}\}$ ,*

$$\mathbb{P} \left( \lim_{L_{\text{te}} \rightarrow \infty} \hat{y}_q = \langle \mathbf{w}, \mathbf{x}_q \rangle \right) = 0.$$

The above negative result, whose proof is found in Appendix B, lays the motivation behind examining more complex and deeper architectures for the data distribution provided herein. Zhang et al. [2024a] demonstrate, for a particular shifting-covariate distribution, that the LSA model with weights obtained via gradient flow fails to in-context learn. In contrast, Theorem 4.1 establishes a negative result in full generality, showing that no parameter configuration will yield success at the ICL task under the multi-modal setting.

## 5 A Multi-layer CA Model

Motivated by Theorem 4.1, we propose a model where the embedding matrix is now learned and obtained from a deep network of layers akin to CA. Consider the model

$$\hat{y}_q = \text{SA}(\mathbf{E}_F; \theta)_{d+1, L+1} \quad \text{where} \quad \mathbf{E}_F := \begin{bmatrix} \mathbf{F} & \mathbf{x}_q \\ \mathbf{y}^\top & 0 \end{bmatrix} \tag{5.1}$$

$$\text{and} \quad \mathbf{F} := \text{CA}(\mathbf{X}; \gamma).$$

The above model (5.1) is a composition of a self-attention layer applied to an embedding  $\mathbf{E}_F$  that is in turn obtained by applying multiple layers of CA between the covariates  $\mathbf{X}$  and an evolving distribution  $\{\mathbf{F}_t\}_{t \geq 0}$  defined below. The final SA layer is defined analogously to (4.3) with parameters  $\theta$  and where  $\mathbf{E}_F$  now replaces  $\mathbf{E}_X$ . Now, to define the CA model  $\text{CA}(\mathbf{X}; \gamma)$ , consider the recurrence

$$\mathbf{F}_t = \mathbf{F}_{t-1} + \mathbf{S}_{t-1} + \mathbf{A}_{t-1} \tag{5.2}$$

<sup>1</sup>For instance, any distribution on  $\mathbf{m}$  that is absolutely continuous with respect to the Lebesgue measure in  $\mathbb{R}^d$ .

for  $t = 1, \dots, T$  where  $\mathbf{A}_{t-1}$  is the output of an attention head,

$$\begin{aligned} \mathbf{A}_{t-1} &= \text{A}(\mathbf{Q}_{t-1}, \mathbf{K}_{t-1}, \mathbf{V}_{t-1}) \\ &= \mathbf{V}_{t-1} \cdot \text{softmax}\left(\frac{\mathbf{K}_{t-1}^\top \mathbf{Q}_{t-1}}{L}\right), \end{aligned} \quad (5.3)$$

with

$$\mathbf{V}_{t-1} = \mathbf{W}_{t-1}^V \mathbf{X}, \quad \mathbf{K}_{t-1} = \mathbf{W}_{t-1}^K \mathbf{X}, \quad \mathbf{Q}_{t-1} = \mathbf{W}_{t-1}^Q \mathbf{F}_{t-1}$$

where  $\mathbf{W}_{t-1}^V, \mathbf{W}_{t-1}^K, \mathbf{W}_{t-1}^Q$  are learnable weight matrices, and

$$\mathbf{S}_{t-1} = \mathbf{W}_{t-1}^S \mathbf{X}$$

with learnable weight matrix  $\mathbf{W}_{t-1}^S$ . We take  $\mathbf{F}_0 = 0_{d \times L}$  to begin the recurrence and set  $\mathbf{F} = \mathbf{F}_T$  with  $T$  denoting the depth of the CA embedding. The weights of the embedding are  $\gamma = \{\mathbf{W}_t^V, \mathbf{W}_t^K, \mathbf{W}_t^Q, \mathbf{W}_t^S\}_{t=0}^{T-1}$ .

Notice that since the query matrix  $\mathbf{Q}_{t-1}$  depends on  $\mathbf{F}_{t-1}$ ,  $\mathbf{A}_{t-1}$  is an application of CA between the original data matrix  $\mathbf{X}$  and an evolving data distribution  $\mathbf{F}_{t-1}$ . For this reason, we view (5.1) as a  $T$ -layer CA model followed by a single layer of SA to obtain the final model output. The model includes the skip-connection of the previous layer input  $\mathbf{F}_{t-1}$  in each layer (5.2) resembling standard transformers. Diverging from conventional architectures [Vaswani et al., 2017], we also include a learnable skip-connection  $\mathbf{S}_{t-1}$  that injects the unaltered raw data  $\mathbf{X}$  into each layer as displayed in Figure 1. Taking inspiration from unrolled neural networks [Gregor and LeCun, 2010, Monga et al., 2021], the inclusion of  $\mathbf{S}_{t-1}$  was preceded by theoretical considerations—specifically, to yield embeddings  $\mathbf{E}_F$  with desirable properties—and later supported by ablation experiments (see Appendix F). As earlier, we use the bottom-right corner of the final output as our prediction  $\hat{y}_q$ . To ensure the analysis remains tractable, we replace the `softmax` with an identity map along the lines of Section 4.2 and prior theoretical literature on ICL [Von Oswald et al., 2023, Ahn et al., 2023, Zhang et al., 2024a, Lu et al., 2025]. This yields the linearization

$$\hat{y}_q = \text{LSA}(\mathbf{E}_F; \theta)_{d+1, L+1} \quad \text{where} \quad \mathbf{E}_F = \begin{bmatrix} \mathbf{F} & \mathbf{x}_q \\ \mathbf{y}^\top & 0 \end{bmatrix} \quad (5.4)$$

$$\text{and} \quad \mathbf{F} = \text{LCA}(\mathbf{X}; \gamma)$$

where the  $\text{LCA}(\mathbf{X}; \gamma)$  simply denotes  $\text{CA}(\mathbf{X}; \gamma)$  whereby (5.3) is modified to

$$\text{A}(\mathbf{Q}_{t-1}, \mathbf{K}_{t-1}, \mathbf{V}_{t-1}) = \mathbf{V}_{t-1} \cdot \frac{\mathbf{K}_{t-1}^\top \mathbf{Q}_{t-1}}{L}.$$

For mathematical simplification, we do not include two key components of conventional transformers—layer normalization [Xiong et al., 2020] and non-linear activations (MLP layers). That said, the model (5.4) is highly-nonlinear in  $\mathbf{X}$  and the final LSA readout is itself a non-linear (cubic) transformation of the learned embedding  $\mathbf{E}_F$ . Additionally, we notice qualitative similarities between the minima both with and without layer normalization (see Figure 6, Appendix G).

## 5.1 Weight Simplifications

Thus far, the learnable weights have remained unconstrained. We now restrict their parameter space to ensure analytical tractability. To this end, we consider two simplifications. For both, we freeze

$$\begin{aligned} \mathbf{W}_{t-1}^K &= \mathbf{W}_{t-1}^Q = \mathbf{I}_d, \quad \mathbf{W}^{PV} = \begin{bmatrix} \mathbf{0}_{d \times d} & \mathbf{0}_d \\ \mathbf{0}_d^\top & 1 \end{bmatrix}, \\ \text{and} \quad \mathbf{W}^{KQ} &= \begin{bmatrix} \mathbf{I}_d & \mathbf{0}_d \\ \mathbf{0}_d^\top & 0 \end{bmatrix}. \end{aligned}$$

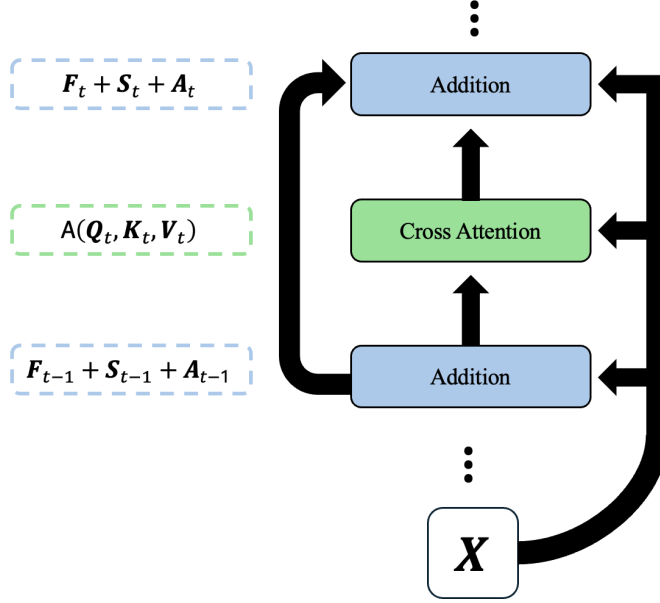


Figure 1: Visual representation of the re-injection of covariates  $\mathbf{X}$  throughout the CA (LCA) embedding in addition to the skip-connection  $\mathbf{F}_t$  standard to transformers [Vaswani et al., 2017]. The propagation of the raw data  $\mathbf{X}$  occurs both through  $\mathbf{S}_t$  as well as through the CA block  $\mathbf{A}_t$ .

We note that the prescription of zero blocks in  $\mathbf{W}^{PV}$  and  $\mathbf{W}^{KQ}$  mimics the initialization given in [Zhang et al., 2024a].

**One-parameter Model.** In the first case, we tie weights across layers and set

$$\mathbf{W}_{t-1}^S = -\mathbf{W}_{t-1}^V = \alpha \mathbf{I}_d \quad (5.5)$$

for all  $0 \leq t \leq T - 1$  where  $\alpha \in \mathbb{R}$  is a learnable scalar parameter. This gives a one-parameter model

$$\hat{y}_q = f(\mathbf{X}, \mathbf{x}_q, \mathbf{y}; \alpha).$$

**Two-parameter Model.** For the second model, we instead set

$$\mathbf{W}_{t-1}^S = \alpha \mathbf{I}_d \quad \text{and} \quad \mathbf{W}_{t-1}^V = \beta \mathbf{I}_d \quad (5.6)$$

for all  $0 \leq t \leq T - 1$  where  $(\alpha, \beta) \in \mathbb{R}^2$  are learnable parameters, yielding a two-parameter model

$$\hat{y}_q = f(\mathbf{X}, \mathbf{x}_q, \mathbf{y}; \alpha, \beta).$$

The first model is recovered from the second by setting  $\beta = -\alpha$ . In both cases, we have kept the original architecture while restricting the parameter space. Assuming a well-chosen training procedure, one can thus view the performance of the one- and two-parameter models as an upper-bound for the full model where all parameters are free. We show in the following that the two simplified models successfully achieve Bayes-optimal prediction in the ICL setting when trained by gradient flow.

## 6 Training Setup and Main Results

### 6.1 Training Setup

Herein, we consider the one- and two-parameter models  $\hat{y}_q = f(\mathbf{X}, \mathbf{x}_q, y; \theta)$  of Section 5.1 where  $\theta$  either denotes the parameters  $\alpha$  or  $(\alpha, \beta)$ . Starting with a set of  $N$  training prompts  $\{(\mathbf{x}_i^{(j)}, y_i^{(j)})_{i=1}^{L_{\text{tr}}} \cup (\mathbf{x}_q^{(j)}, y_q^{(j)})\}_{j=1}^N$ , given real-valued, continuous targets, it is natural to consider the empirical squared loss on the target query

$$\ell_{N, L_{\text{tr}}}(\theta) := \frac{1}{N} \sum_{j=1}^N \left( y_q^{(j)} - f(\mathbf{X}^{(j)}, \mathbf{x}_q^{(j)}, y^{(j)}; \theta) \right)^2.$$

As in prior work [Zhang et al., 2024a, Ahn et al., 2023], taking the number of training prompts  $N \rightarrow \infty$ , we operate on the population loss

$$\ell_{L_{\text{tr}}}(\theta) := \lim_{N \rightarrow \infty} \ell_{N, L_{\text{tr}}}(\theta) = \mathbb{E} \left[ (y_q - f(\mathbf{X}, \mathbf{x}_q, \mathbf{y}; \theta))^2 \right],$$

where the expectation is taken with respect to the joint distribution detailed in Section 3. As a final reduction, we consider the asymptotic, training context-length regime and define the loss

$$\ell(\theta) := \lim_{L_{\text{tr}} \rightarrow \infty} \ell_{L_{\text{tr}}}(\theta).$$

This regime is qualitatively similar to prior work [Zhang et al., 2024a] whereby one establishes the ICL capacity of the model at large context length, however our presentation diverges by taking the  $L_{\text{tr}} \rightarrow \infty$  limit before training on the loss function.

Having established the loss of interest, the training procedure for both variants of the CA model will simply be to run gradient flow on the limiting objective  $\ell$ . That is, the model parameters evolve according to the ordinary differential equation

$$\frac{d}{dt} \theta_t = -\nabla \ell(\theta_t),$$

where  $(\theta_t)_{t \geq 0}$  is the trajectory of the parameters over the training horizon. Gradient flow can be seen as the limit of gradient descent in vanishing step size. Analyzing optimization in the gradient flow limit has enabled precise characterization of deep neural network training dynamics [Saxe et al., 2013, Chizat and Bach, 2018]; this approach has been leveraged in previous studies on ICL for transformers [Zhang et al., 2024a, 2025].

### 6.2 Main Results

Recall the stacked modality-dependent vector  $\mathbf{m}$  from (3.2). We make the following assumption on the distribution of  $\mathbf{m}$  across prompts.

**Assumption 6.1** (Support of  $\|\mathbf{m}\|$ ). Assume  $\mathbf{m}$  has a continuous distribution and

$$\underline{m} := \text{ess inf } \|\mathbf{m}\|^2 < \text{ess sup } \|\mathbf{m}\|^2 =: \bar{m} < \infty$$

so that  $\|\mathbf{m}\|$  is almost-surely bounded and non-degenerate.

The boundedness assumption on  $\mathbf{m}$  is mild. For example, it holds as soon as the covariates are normalized, for instance  $\mathbf{x}_i \in [0, 1]^d$ . The density assumption is included for technical reasons; it simplifies the proofs of our main results. We do not believe this assumption is intrinsically necessary for the results described below.

We now present our main results. We show that a deep model of CA layers learns the Bayes-optimal prediction rule in-context for this multi-modal problem.

**Theorem 6.2** (One-parameter model optimality). *Run gradient flow on the loss  $\ell(\alpha)$  for the one-parameter model. Under the data generating process in Section 3 and Assumption 6.1, we have:*

1. *Gradient flow converges. Formally, letting  $(\alpha_{t,T})_{t \geq 0}$  denote the gradient flow trajectory for a CA stack of depth  $T$ , the limit  $\alpha_T^* := \lim_{t \rightarrow \infty} \alpha_{t,T}$  exists.*

2. *As  $T \rightarrow \infty$ ,*

$$\alpha_T^* \rightarrow \frac{2}{2 + \underline{m} + \overline{m}} =: \alpha^*.$$

3. *The resulting predictor is Bayes optimal as the depth diverges. Formally,*

$$\lim_{T \rightarrow \infty} \lim_{L_{te} \rightarrow \infty} \hat{y}_q = \langle \mathbf{w}, \mathbf{x}_q \rangle$$

*almost surely.*

We prove this result in Appendix D. We sketch the proof ideas below.

*Proof sketch.* The one-parameter loss assumes the compact form

$$\ell(\alpha) = \mathbb{E} \left[ \frac{\|\mathbf{m}\|^2}{1 + \|\mathbf{m}\|^2} (1 - \alpha(\|\mathbf{m}\|^2 + 1))^{2T} \right]$$

up to an additive constant independent of  $\alpha$ . The strict convexity and coercivity of this loss imply convergence of gradient flow using well-established theory [Garrigos and Gower, 2023]. Subsequently, taking the  $(\cdot)^{1/2T}$ -th root of the loss, one shows epigraphical convergence [Rockafellar and Wets, 1998] as  $T \rightarrow \infty$  to the limit

$$\phi(\alpha) = \max\{|1 - \alpha(\underline{m} + 1)|, |1 - \alpha(\overline{m} + 1)|\}.$$

This yields convergence of the sequence of minimizers  $(\alpha_T^*)_{T \geq 1}$  to the unique minimizer of  $\phi$  which is merely  $\alpha^*$ . Bayes optimality follows by solving the recurrence 5.2 to find that

$$\lim_{L_{te} \rightarrow \infty} \hat{y}_q = \langle \mathbf{w}, \mathbf{x}_q \rangle + e(\alpha) \tag{6.1}$$

with error  $e(\alpha) = O(\|\mathbf{I} - \alpha \mathbf{\Lambda}\|^T)$  where  $\|\mathbf{I} - \alpha \mathbf{\Lambda}\| < 1$  at  $\alpha = \alpha^*$  and hence  $e(\alpha^*) \rightarrow 0$  as  $T \rightarrow \infty$ .  $\square$

We now turn to the two-parameter setting in the following result which requires additional technical assumptions.

**Theorem 6.3** (Two-parameter model optimality). *Under the data generating process in Section 3, Assumption 6.1, and the regularity condition of Remark E.4, run gradient flow on the loss  $\ell(\alpha, \beta)$  for the two-parameter model with initialization*

$$\beta_0 \in (-2/(\overline{m} + 1), 0) \quad \text{and} \quad \alpha_0 = \alpha^*(\beta_0) \tag{6.2}$$

where  $\beta \mapsto \alpha^*(\beta)$  is defined in Appendix E.1. Then, we have the following:

1. *Gradient flow converges. Formally, letting  $(\alpha_{t,T}, \beta_{t,T})_{t \geq 0}$  denote the gradient flow trajectory for a CA stack of depth  $T$ , the limit  $(\alpha_T^*, \beta_T^*) := \lim_{t \rightarrow \infty} (\alpha_{t,T}, \beta_{t,T})$  exists.*

2. *Suppose  $\lim_{T \rightarrow \infty} \beta_T^* \notin \{-2/(\overline{m} + 1), 0\}$ . Then, with  $\alpha^*$  as defined in Theorem 6.2, as  $T \rightarrow \infty$ ,*

$$\alpha_T^* \rightarrow \alpha^*$$

*and*

$$\beta_T^* \rightarrow -\alpha^*.$$

3. Under the same hypothesis as above, as in Theorem 6.2, the resulting predictor is Bayes optimal as the depth grows. Formally,

$$\lim_{T \rightarrow \infty} \lim_{L_{te} \rightarrow \infty} \hat{y}_q = \langle \mathbf{w}, \mathbf{x}_q \rangle$$

almost surely.

As before, we include a brief sketch of the proof of Theorem 6.3. This will also motivate the choice of the initialization in the theorem above.

*Proof sketch.* The two-parameter loss has the explicit expression

$$\ell(\alpha, \beta) = \mathbb{E} \left[ \frac{\|\mathbf{m}\|^2}{1 + \|\mathbf{m}\|^2} \left( \frac{\alpha}{\beta} [(1 + \beta(\|\mathbf{m}\|^2 + 1))^T - 1] - 1 \right)^2 \right].$$

This loss is non-convex and non-coercive; however, it is quadratic in  $\alpha$  for fixed  $\beta$  with profiled minimizer  $\alpha^*(\beta) = \operatorname{argmin}_{\alpha \in \mathbb{R}} \ell(\alpha, \beta)$ . By using this structure, we first show that  $(\alpha_t)_{t \geq 0}$  (at fixed depth  $T$ ) is bounded. Then, establishing that

$$\ell(\alpha_0, \beta_0) < \inf_{\alpha \in \mathbb{R}} \min\{\ell(\alpha, -2/(\overline{m} + 1)), \ell(\alpha, 0)\}$$

and given gradient flow is characteristically non-increasing on the loss  $\ell(\alpha, \beta)$ , it follows that  $(\beta_t)_{t \geq 0} \subset (-2/(\overline{m} + 1), 0)$ —namely the entire gradient flow trajectory  $(\alpha_t, \beta_t)_{t \geq 0}$  remains bounded. Starting with this a priori boundedness, we establish convergence of gradient flow at fixed  $T$ . To determine the limiting behavior as  $T \rightarrow \infty$ , one takes a log-transformation of  $\beta \mapsto \ell(\alpha^*(\beta), \beta)$  and finds that its derivative remains nonzero for sufficiently large  $T$  if  $\lim_{T \rightarrow \infty} \beta_T^* \neq -\alpha^*$ . This contradicts  $(\alpha_T^*, \beta_T^*)_{T \geq 1}$  being a sequence of stationary points. Convergence of  $\alpha_T^* \rightarrow \alpha^*$  as  $T \rightarrow \infty$  follows by examining  $\lim_{T \rightarrow \infty} \alpha^*(\beta_T)$  as necessarily  $\alpha_T^* = \alpha^*(\beta_T^*)$ . Finally, Bayes optimality is delivered via the same argument as in Theorem 6.2.  $\square$

The proof of the above result is considerably more intricate than that of Theorem 6.2 and can be found in Appendix E. Theorem 6.3 shows that the limiting behavior of the two-parameter model mimics that of the one-parameter setting, whereby in both cases one achieves the Bayes-optimal predictor.

A careful reader may have noticed how the proof sketches above help inform the choice of initialization (6.2). Firstly, a short calculation shows that

$$\alpha \in (0, 2/(\overline{m} + 1)) \implies \|\mathbf{I} - \alpha \mathbf{\Lambda}\| < 1 \tag{6.3}$$

almost surely. Therefore, from (6.1), choosing any  $\alpha$  in this window for the one-parameter setup (6.3) will produce a Bayes-optimal prediction. Given the correspondence between the two models (see (5.5) and (5.6)), this lends to  $\beta_0 \in (-2/(\overline{m} + 1), 0)$  as a suitable initialization in the two-parameter setup. Moreover, as  $\ell(\alpha, \beta)$  is quadratic in  $\alpha$  with explicit minimizer  $\alpha^*(\beta)$ , starting at  $\alpha_0 = \alpha^*(\beta_0)$  becomes an obvious choice. This intuition is supported in a visualization of the loss landscape provided in Figure 6, Appendix G.

### 6.3 The limiting parameter $\alpha^*$

Thus far, we have only mentioned that the limiting parameter  $\alpha^* = 2/(2 + \underline{m} + \overline{m})$  suffices for Bayes optimality—which follows from (6.1) and (6.3)—but have not commented on its particular form. As remarked above, for the one-parameter model, one learns the ICL task at asymptotic depth if  $\|\mathbf{I} - \alpha \mathbf{\Lambda}\| < 1$  with vanishing error  $\epsilon(\alpha)$ . Recalling  $\mathbf{\Lambda} = \mathbf{I} + \underline{m} \mathbf{m}^\top$ , along the spike direction, the absolute value of the largest attainable eigenvalue is

$$\phi(\alpha) := \max\{|1 - \alpha(1 + \underline{m})|, |1 - \alpha(1 + \overline{m})|\}$$

and we note  $\alpha^* = \operatorname{argmin}_{\alpha \in \mathbb{R}} \phi(\alpha)$ . Interestingly, the limiting parameter  $\alpha^*$  coincides with the parametrization minimizing the worst-case error rate given by the spike contribution to  $e(\alpha)$ . Hence, Theorems 6.2 and 6.3 show that the CA models are in a sense minimax optimal in the large  $T$  and  $L_{\text{te}}$  limits.

## 6.4 The role of depth

Consider the embedding  $\mathbf{F} = \text{LCA}(\mathbf{X}; \gamma)$  produced by the  $T$ -layer CA stack, and let  $\{\mathbf{f}_i\}_{i=1}^{L_{\text{te}}}$  denote its columns. Under mild conditions (and ignoring lower-order terms that vanish as  $L_{\text{te}} \rightarrow \infty$ ), the final prediction produced by the LSA readout has the schematic form

$$\hat{y}_q \approx \mathbf{w}^\top \left( \frac{1}{L_{\text{te}}} \sum_{i=1}^{L_{\text{te}}} \mathbf{x}_i \mathbf{f}_i^\top \right) \mathbf{x}_q.$$

as shown in Appendix C (Lemma C.1). Thus, if the CA stack can enforce

$$\frac{1}{L_{\text{te}}} \sum_{i=1}^{L_{\text{te}}} \mathbf{x}_i \mathbf{f}_i^\top \longrightarrow \mathbf{I}_d \quad \text{as } T \rightarrow \infty, \quad (6.4)$$

then  $\hat{y}_q \rightarrow \langle \mathbf{w}, \mathbf{x}_q \rangle$  as both  $T \rightarrow \infty$  and  $L_{\text{te}} \rightarrow \infty$ , yielding Bayes-optimal ICL. An instance where (6.4) can occur is if

$$\mathbf{F} \approx \mathbf{\Lambda}^{-1} \mathbf{X} \quad (6.5)$$

—that is, the embedding  $\mathbf{F}$  whitens the covariates. Crucially, since the embedding  $\mathbf{F}$  is prompt-dependent, (6.5) is achievable even though  $\mathbf{\Lambda}$  is random: the model is not constrained to learning a single global inverse covariance, instead it can compute  $\mathbf{\Lambda}^{-1}$  implicitly from the prompt itself. Here lies the significance of the CA embedding as a whitening (denoising) mechanism for the covariates.

We note that in sharp contrast to the mechanism above, a single LSA layer can only learn an average covariance, and thus fails to attain Bayes-optimal performance in our setup.

## 7 Numerical Experiments

To convey the insights of Theorems 4.1, 6.2, and 6.3 in a more accessible form, we provide the results of some numerical experiments, now opting for gradient descent in place of its continuous analog and operating on the non-asymptotic objective  $\ell_{N, L_{\text{tr}}}$ . In Figure 2, we observe the failure of the single-layer LSA model proved in Theorem 4.1. In contrast, LCA-based models achieve error-rates which are several orders of magnitude smaller as  $L_{\text{te}}$  grows. Figure 3 shows the effect of depth in the LCA embedding in aiding model performance on the multi-modal ICL task. Notably, despite the asymptotic presentation of Theorems 6.2 and 6.3, we observe exceptional performance at moderate depth as anticipated by the geometric-rate error decay (6.1).

## 8 Discussion

We studied a multi-modal task in which each prompt is generated by a latent factor model, inducing prompt-dependent covariate statistics which place the setting outside of standard unimodal ICL analyses. To elucidate this added complexity, we first demonstrated the failure of single-layer LSA models standard in the literature. Motivated by this limitation, we introduced a novel transformer-like architecture, incorporating both depth and CA, proving not only its expressibility for the ICL task, but also demonstrating its capacity to learn the Bayes-optimal predictor via gradient flow.

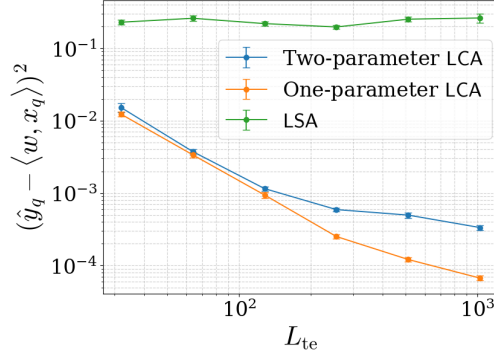


Figure 2: In-context performance at various  $L_{te}$  of one- and two-parameter LCA-based models ( $T = 10$ ) and LSA model from (4.2). Models are optimized on  $\ell_{N, L_{tr}}$  ( $L_{tr} = 100, N = 2000$ ) using gradient descent. Error bars represent standard deviation over 1000 test-prompts.

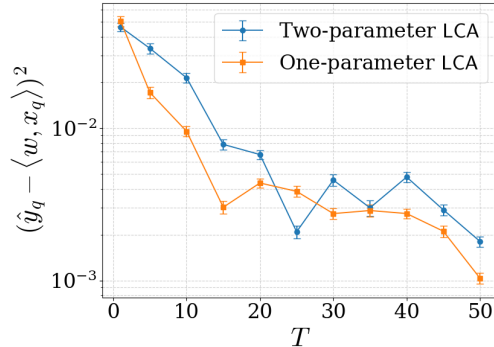


Figure 3: In-context performance for  $L_{te} = 64$  at various  $T$  of one- and two-parameter LCA models. Models are optimized on  $\ell_{N, L_{tr}}$  ( $L_{tr} = 100, N = 2000$ ) using gradient descent. Error bars represent standard deviation over 1000 test-prompts.

To our knowledge, our work is the first to tackle a multi-modal ICL task in a mathematically tractable setting and provably overcome covariate distribution shifts among prompts. Continuing on the theoretical side, a natural future direction will include exploring models where the covariance structure contains more than one spike—that is, generalizations of (3.4). Additionally, it will be of interest to study if the learnable weights can be varied over larger parameter classes, and whether a similar collapse as seen for the two-parameter to one-parameter case is observed for more complex settings.

Toward applications, the CA architecture proposed in (5.2) is novel and should be tested on real-world, multi-modal data without the linearization and with all the conventional sophistications of modern large-language models.

Lastly, while we analyzed the population loss for our CA architecture, it would be significant to extend this to sample-level results, as done earlier for unimodal problems [Lu et al., 2025]. In addition, extending to infinite token dimensions, in the spirit of [Lu et al., 2025, Letey et al., 2025], would also constitute a crucial direction for future research. These directions pose intriguing mathematical challenges, in particular, requiring potential new developments in random matrix theory, which we view as an exciting follow-up to

the present paper.

## Acknowledgments

N.B. acknowledges support from the *Fonds de recherche du Québec—Nature et technologies* (FRQNT). S.S. gratefully acknowledges support from the National Science Foundation (DMS CAREER 2239234), Office of Naval Research (N00014-23-1-2489) and Air Force Office of Scientific Research (FA9950-23-1-0429). P.S. was partially funded by the National Science Foundation (DMS CAREER 2440824).

## References

- Kwangjun Ahn, Xiang Cheng, Hadi Daneshmand, and Suvrit Sra. Transformers learn to implement pre-conditioned gradient descent for in-context learning. In *Thirty-seventh Conference on Neural Information Processing Systems*, 2023.
- Ekin Akyürek, Dale Schuurmans, Jacob Andreas, Tengyu Ma, and Denny Zhou. What learning algorithm is in-context learning? investigations with linear models. In *The Eleventh International Conference on Learning Representations*, 2023.
- Jean-Baptiste Alayrac, Jeff Donahue, Pauline Luc, Antoine Miech, Iain Barr, Yana Hasson, Karel Lenc, Arthur Mensch, Katherine Millican, Malcolm Reynolds, Roman Ring, Eliza Rutherford, Serkan Cabi, Tengda Han, Zhitao Gong, Sina Samangooei, Marianne Monteiro, Jacob Menick, Sebastian Borgeaud, Andrew Brock, Aida Nematzadeh, Sahand Sharifzadeh, Mikolaj Binkowski, Ricardo Barreira, Oriol Vinyals, Andrew Zisserman, and Karen Simonyan. Flamingo: a visual language model for few-shot learning. In Alice H. Oh, Alekh Agarwal, Danielle Belgrave, and Kyunghyun Cho, editors, *Advances in Neural Information Processing Systems*, 2022.
- Luca Arnaboldi, Bruno Loureiro, Ludovic Stephan, Florent Krzakala, and Lenka Zdeborova. Asymptotics of SGD in sequence-single index models and single-layer attention networks. In *The Thirty-ninth Annual Conference on Neural Information Processing Systems*, 2025.
- Yu Bai, Fan Chen, Huan Wang, Caiming Xiong, and Song Mei. Transformers as statisticians: Provable in-context learning with in-context algorithm selection. In *Workshop on Efficient Systems for Foundation Models @ ICML2023*, 2023.
- Nicholas Barnfield, Hugo Cui, and Yue M Lu. High-dimensional analysis of single-layer attention for sparse-token classification. *arXiv preprint arXiv:2509.25153*, 2025.
- Tom Brown, Benjamin Mann, Nick Ryder, Melanie Subbiah, Jared D Kaplan, Prafulla Dhariwal, Arvind Neelakantan, Pranav Shyam, Girish Sastry, Amanda Askell, et al. Language models are few-shot learners. *Advances in neural information processing systems*, 33:1877–1901, 2020.
- Tianxi Cai, Feiqing Huang, Ryumei Nakada, Linjun Zhang, and Doudou Zhou. Contrastive learning on multimodal analysis of electronic health records. *arXiv preprint arXiv:2403.14926*, 2024.
- Siyu Chen, Heejune Sheen, Tianhao Wang, and Zhuoran Yang. Training dynamics of multi-head softmax attention for in-context learning: Emergence, convergence, and optimality. *arXiv preprint arXiv:2402.19442*, 2024.

- Michelle Ching, Ioana Popescu, Nico Smith, Tianyi Ma, William G Underwood, and Richard J Samworth. Efficient and minimax-optimal in-context nonparametric regression with transformers. *arXiv preprint arXiv:2601.15014*, 2026.
- Lenaic Chizat and Francis Bach. On the global convergence of gradient descent for over-parameterized models using optimal transport. *Advances in neural information processing systems*, 31, 2018.
- Haotian Cui, Alejandro Tejada-Lapuerta, Maria Brbić, Julio Saez-Rodriguez, Simona Cristea, Hani Goodarzi, Mohammad Lotfollahi, Fabian J Theis, and Bo Wang. Towards multimodal foundation models in molecular cell biology. *Nature*, 640(8059):623–633, 2025.
- Hugo Cui, Freya Behrens, Florent Krzakala, and Lenka Zdeborová. A phase transition between positional and semantic learning in a solvable model of dot-product attention. *Advances in Neural Information Processing Systems*, 37:36342–36389, 2024.
- Yash Deshpande, Subhabrata Sen, Andrea Montanari, and Elchanan Mossel. Contextual stochastic block models. *Advances in Neural Information Processing Systems*, 31, 2018.
- Daisy Yi Ding, Shuangning Li, Balasubramanian Narasimhan, and Robert Tibshirani. Cooperative learning for multiview analysis. *Proceedings of the National Academy of Sciences*, 119(38):e2202113119, 2022.
- Shivam Garg, Dimitris Tsipras, Percy S Liang, and Gregory Valiant. What can transformers learn in-context? a case study of simple function classes. *Advances in neural information processing systems*, 35: 30583–30598, 2022.
- Guillaume Garrigos and Robert M Gower. Handbook of convergence theorems for (stochastic) gradient methods. *arXiv preprint arXiv:2301.11235*, 2023.
- Karol Gregor and Yann LeCun. Learning fast approximations of sparse coding. In *Proceedings of the 27th international conference on international conference on machine learning*, pages 399–406, 2010.
- Yu Gui, Cong Ma, and Zongming Ma. Multi-modal contrastive learning adapts to intrinsic dimensions of shared latent variables. *arXiv preprint arXiv:2505.12473*, 2025.
- Yu Huang, Yuan Cheng, and Yingbin Liang. In-context convergence of transformers. *arXiv preprint arXiv:2310.05249*, 2023.
- Andrew Jaegle, Felix Gimeno, Andy Brock, Oriol Vinyals, Andrew Zisserman, and Joao Carreira. Perceiver: General perception with iterative attention. In *International conference on machine learning*, pages 4651–4664. PMLR, 2021.
- Christian Keup and Lenka Zdeborová. Optimal thresholds and algorithms for a model of multi-modal learning in high dimensions. *Journal of Statistical Mechanics: Theory and Experiment*, 2025(9):093302, 2025.
- Mary I Letey, Jacob A Zavatore-Veth, Yue M Lu, and Cengiz Pehlevan. Pretrain-test task alignment governs generalization in in-context learning. *arXiv preprint arXiv:2509.26551*, 2025.
- Chunyu Li, Zhe Gan, Zhengyuan Yang, Jianwei Yang, Linjie Li, Lijuan Wang, Jianfeng Gao, et al. Multimodal foundation models: From specialists to general-purpose assistants. *Foundations and Trends® in Computer Graphics and Vision*, 16(1-2):1–214, 2024.

- Yingcong Li, Muhammed Emrullah Ildiz, Dimitris Papailiopoulos, and Samet Oymak. Transformers as algorithms: Generalization and stability in in-context learning. In *International conference on machine learning*, pages 19565–19594. PMLR, 2023.
- Xiaohao Liu, Xiaobo Xia, See-Kiong Ng, and Tat-Seng Chua. Continual multimodal contrastive learning. *arXiv preprint arXiv:2503.14963*, 2025.
- Jiasen Lu, Dhruv Batra, Devi Parikh, and Stefan Lee. Vilbert: Pretraining task-agnostic visiolinguistic representations for vision-and-language tasks. *Advances in neural information processing systems*, 32, 2019.
- Yue M Lu, Mary Letey, Jacob A Zavatore-Veth, Anindita Maiti, and Cengiz Pehlevan. Asymptotic theory of in-context learning by linear attention. *Proceedings of the National Academy of Sciences*, 122(28): e2502599122, 2025.
- Tianyi Ma, Tengyao Wang, and Richard J Samworth. Provable test-time adaptivity and distributional robustness of in-context learning. *arXiv preprint arXiv:2510.23254*, 2025.
- Rodrigo Maulen-Soto, Pierre Marion, and Claire Boyer. Attention-based clustering. In *The Thirty-ninth Annual Conference on Neural Information Processing Systems*, 2025.
- Pierre Mergny and Lenka Zdeborová. Spectral thresholds in correlated spiked models and fundamental limits of partial least squares. *arXiv preprint arXiv:2510.17561*, 2025.
- Vishal Monga, Yuelong Li, and Yonina C Eldar. Algorithm unrolling: Interpretable, efficient deep learning for signal and image processing. *IEEE Signal Processing Magazine*, 38(2):18–44, 2021.
- Sagnik Nandy and Zongming Ma. Multimodal data integration and cross-modal querying via orchestrated approximate message passing. *arXiv preprint arXiv:2407.19030*, 2024.
- Samet Oymak, Ankit Singh Rawat, Mahdi Soltanolkotabi, and Christos Thrampoulidis. On the role of attention in prompt-tuning. In *International Conference on Machine Learning*, pages 26724–26768. PMLR, 2023.
- Alec Radford, Jong Wook Kim, Chris Hallacy, Aditya Ramesh, Gabriel Goh, Sandhini Agarwal, Girish Sastry, Amanda Askell, Pamela Mishkin, Jack Clark, et al. Learning transferable visual models from natural language supervision. In *International conference on machine learning*, pages 8748–8763. PMLR, 2021.
- R. Tyrrell Rockafellar and Roger J.-B. Wets. *Variational Analysis*, volume 317 of *Grundlehren der mathematischen Wissenschaften*. Springer, Berlin, Heidelberg, 1998. ISBN 978-3-540-62772-2.
- Andrew M Saxe, James L McClelland, and Surya Ganguli. Exact solutions to the nonlinear dynamics of learning in deep linear neural networks. *arXiv preprint arXiv:1312.6120*, 2013.
- Renat Sergazinov, Armeen Taeb, and Irina Gaynanova. A spectral method for multi-view subspace learning using the product of projections. *Biometrika*, page asaf088, 2025.
- Wei Shen, Ruida Zhou, Jing Yang, and Cong Shen. On the training convergence of transformers for in-context classification of gaussian mixtures. In *Forty-second International Conference on Machine Learning*, 2025.
- Jean-Jacques E Slotine, Weiping Li, et al. *Applied nonlinear control*, volume 199. Prentice hall Englewood Cliffs, NJ, 1991.

- Emanuele Troiani, Hugo Cui, Yatin Dandi, Florent Krzakala, and Lenka Zdeborova. Fundamental limits of learning in sequence multi-index models and deep attention networks: high-dimensional asymptotics and sharp thresholds. In *Forty-second International Conference on Machine Learning*, 2025.
- Ashish Vaswani, Noam Shazeer, Niki Parmar, Jakob Uszkoreit, Llion Jones, Aidan N Gomez, Lukasz Kaiser, and Illia Polosukhin. Attention is all you need. *Advances in neural information processing systems*, 30, 2017.
- Johannes Von Oswald, Eyvind Niklasson, Ettore Randazzo, João Sacramento, Alexander Mordvintsev, Andrey Zhmoginov, and Max Vladymyrov. Transformers learn in-context by gradient descent. In *International Conference on Machine Learning*, pages 35151–35174. PMLR, 2023.
- Zirui Wang, Mengzhou Xia, Luxi He, Howard Chen, Yitao Liu, Richard Zhu, Kaiqu Liang, Xindi Wu, Haotian Liu, Sadhika Malladi, et al. Charxiv: Charting gaps in realistic chart understanding in multimodal llms. *Advances in Neural Information Processing Systems*, 37:113569–113697, 2024.
- Jingfeng Wu, Difan Zou, Zixiang Chen, Vladimir Braverman, Quanquan Gu, and Peter Bartlett. How many pretraining tasks are needed for in-context learning of linear regression? In *The Twelfth International Conference on Learning Representations*, 2024.
- Sang Michael Xie, Aditi Raghunathan, Percy Liang, and Tengyu Ma. An explanation of in-context learning as implicit bayesian inference. In *International Conference on Learning Representations*, 2022.
- Ruibin Xiong, Yunchang Yang, Di He, Kai Zheng, Shuxin Zheng, Chen Xing, Huishuai Zhang, Yanyan Lan, Liwei Wang, and Tieyan Liu. On layer normalization in the transformer architecture. In *International conference on machine learning*, pages 10524–10533. PMLR, 2020.
- Xiaodong Yang, Buyu Lin, and Subhabrata Sen. Fundamental limits of community detection from multi-view data: multi-layer, dynamic and partially labeled block models. *The Annals of Statistics*, 53(6):2728–2756, 2025.
- Ruiqi Zhang, Spencer Frei, and Peter L Bartlett. Trained transformers learn linear models in-context. *Journal of Machine Learning Research*, 25(49):1–55, 2024a.
- Ruiqi Zhang, Jingfeng Wu, and Peter Bartlett. In-context learning of a linear transformer block: Benefits of the MLP component and one-step GD initialization. In *The Thirty-eighth Annual Conference on Neural Information Processing Systems*, 2024b.
- Yedi Zhang, Aaditya K Singh, Peter E. Latham, and Andrew M Saxe. Training dynamics of in-context learning in linear attention. In *Forty-second International Conference on Machine Learning*, 2025.

# A Notation, Basic Identities, and the Bayes-predictor

## A.1 Notation and Conventions

We work with a single prompt (task) unless otherwise stated.

| Symbol  | Meaning   |
|---|---|
| $d = d_1 + d_2$   | total covariate dimension   |
| $L$   | context length (we use $L_{\text{tr}}$ or $L_{\text{te}}$ when needed)                                |
| $\mathbf{x}_i \in \mathbb{R}^d$                                 | stacked covariate for context token $i \in [L]$   |
| $\mathbf{x}_q \in \mathbb{R}^d$                                 | query covariate   |
| $y_i \in \mathbb{R}$  | context response for token $i \in [L]$  |
| $y_q \in \mathbb{R}$  | query response  |
| $\mathbf{m} \in \mathbb{R}^d$                                   | stacked modality vector (prompt-specific), $m = [v; r]$   |
| $\zeta \in \mathbb{R}$  | prompt-specific scalar controlling the response   |
| $u_i \sim \mathcal{N}(0, 1)$                                    | latent scalar shared across modalities and response   |
| $\boldsymbol{\mu}_i \sim \mathcal{N}(0, \mathbf{I}_d)$          | stacked noise in covariates   |
| $\boldsymbol{\Lambda} = \mathbf{I} + \mathbf{m}\mathbf{m}^\top$ | covariate covariance conditional on $\mathbf{m}$  |
| $\boldsymbol{\Sigma}$   | joint covariance of $(x, y)$ conditioned on $(m, \zeta)$  |
| $Z := 1 + \ \mathbf{m}\ ^2$                                     | top eigenvalue of $\boldsymbol{\Lambda}$ (rank-one spike)   |
| $\mathbf{w} \in \mathbb{R}^d$                                   | Bayes-optimal regression coefficient: $\mathbf{w} = \frac{\zeta}{1 + \ \mathbf{m}\ ^2} \mathbf{m}$    |
| $\underline{m}, \bar{m}$  | $\underline{m} = \text{ess inf } \ \mathbf{m}\ ^2$ , $\bar{m} = \text{ess sup } \ \mathbf{m}\ ^2$     |
| $\underline{Z}, \bar{Z}$  | $\underline{Z} = 1 + \underline{m} = \text{ess inf } Z$ , $\bar{Z} = 1 + \bar{m} = \text{ess sup } Z$ |

For two sequences  $(a_n)_{n \geq 1}$  and  $(b_n)_{n \geq 1}$ , we write

$$a_n = O(b_n)$$

to mean  $a_n \leq C \cdot b_n$  for some constant  $C > 0$  for  $n$  sufficiently large. We also use  $o(1)$  to denote a sequence of terms which vanish as the ambient index grows. For example, writing  $a_n = o(1)$  implies  $a_n \rightarrow 0$  as  $n \rightarrow \infty$ .

## A.2 Joint Gaussian Form and Bayes-predictor

Recall the data generating process (Section 3): for  $i \in [L] \cup \{q\}$ ,

$$\mathbf{x}_i = u_i \mathbf{m} + \boldsymbol{\mu}_i, \quad y_i = \zeta u_i,$$

with  $u_i \sim \mathcal{N}(0, 1)$  and  $\boldsymbol{\mu}_i = [\boldsymbol{\xi}_i, \boldsymbol{\eta}_i] \sim \mathcal{N}(0, \mathbf{I}_d)$  independent across tokens  $i$  and independent of  $(\mathbf{m}, \zeta)$ .

**Lemma A.1** (Joint covariance and Bayes coefficient). *Conditional on  $(\mathbf{m}, \zeta)$ , the pair  $(\mathbf{x}_i, y_i) \in \mathbb{R}^{d+1}$  is jointly Gaussian with mean 0 and covariance*

$$\boldsymbol{\Sigma} = \begin{bmatrix} \boldsymbol{\Lambda} & \zeta \mathbf{m} \\ \zeta \mathbf{m}^\top & \zeta^2 \end{bmatrix}, \quad \boldsymbol{\Lambda} = \mathbf{I} + \mathbf{m}\mathbf{m}^\top.$$

Moreover,

$$\mathbb{E}[y_i \mid \mathbf{m}, \zeta, \mathbf{x}_i] = \mathbf{w}^\top \mathbf{x}_i, \quad \mathbf{w} = \frac{\zeta}{1 + \|\mathbf{m}\|^2} \mathbf{m},$$

and we may write

$$y_i = \langle \mathbf{w}, \mathbf{x}_i \rangle + \varepsilon_i, \quad \varepsilon_i \perp\!\!\!\perp \mathbf{x}_i \mid (\mathbf{m}, \zeta), \quad \varepsilon_i \sim \mathcal{N}\left(0, \frac{\zeta^2}{1 + \|\mathbf{m}\|^2}\right).$$

*Proof.* We compute conditional covariances given  $(\mathbf{m}, \zeta)$ :

$$\boldsymbol{\Sigma}_{x,x} := \mathbb{E}[\mathbf{x}_i \mathbf{x}_i^\top \mid \mathbf{m}, \zeta] = \mathbb{E}[(u_i \mathbf{m} + \boldsymbol{\mu}_i)(u_i \mathbf{m} + \boldsymbol{\mu}_i)^\top] = \mathbf{m} \mathbf{m}^\top + \mathbf{I} = \boldsymbol{\Lambda},$$

$$\boldsymbol{\Sigma}_{x,y} := \mathbb{E}[\mathbf{x}_i y_i \mid \mathbf{m}, \zeta] = \mathbb{E}[(u_i \mathbf{m} + \boldsymbol{\mu}_i) \cdot \zeta u_i] = \zeta \mathbb{E}[u_i^2] \mathbf{m} = \zeta \mathbf{m},$$

$$\boldsymbol{\Sigma}_{y,y} := \mathbb{E}[y_i^2 \mid \mathbf{m}, \zeta] = \zeta^2 \mathbb{E}[u_i^2] = \zeta^2,$$

yielding the stated  $\boldsymbol{\Sigma}$ . For a jointly Gaussian vector, the conditional mean is

$$\mathbb{E}[y_i \mid \mathbf{x}_i, \mathbf{m}, \zeta] = \boldsymbol{\Sigma}_{x,y}^\top \boldsymbol{\Sigma}_{x,x}^{-1} \mathbf{x}_i = (\zeta \mathbf{m})^\top \boldsymbol{\Lambda}^{-1} \mathbf{x}_i$$

and so  $\mathbf{w} = \boldsymbol{\Lambda}^{-1}(\zeta \mathbf{m})$ . Using the Sherman–Morrison formula,

$$\boldsymbol{\Lambda}^{-1} = (\mathbf{I} + \mathbf{m} \mathbf{m}^\top)^{-1} = \mathbf{I} - \frac{\mathbf{m} \mathbf{m}^\top}{1 + \|\mathbf{m}\|^2}.$$

and hence,

$$\mathbf{w} = \left( \mathbf{I} - \frac{\mathbf{m} \mathbf{m}^\top}{1 + \|\mathbf{m}\|^2} \right) \zeta \mathbf{m} = \zeta \mathbf{m} - \zeta \frac{\|\mathbf{m}\|^2}{1 + \|\mathbf{m}\|^2} \mathbf{m} = \frac{\zeta}{1 + \|\mathbf{m}\|^2} \mathbf{m}.$$

Finally, the conditional variance of  $y_i$  given  $\mathbf{x}_i$  is

$$\begin{aligned} \text{Var}(y_i \mid \mathbf{x}_i, \mathbf{m}, \zeta) &= \boldsymbol{\Sigma}_{y,y} - \boldsymbol{\Sigma}_{x,y}^\top \boldsymbol{\Sigma}_{x,x}^{-1} \boldsymbol{\Sigma}_{x,y} \\ &= \zeta^2 - (\zeta \mathbf{m})^\top \boldsymbol{\Lambda}^{-1} (\zeta \mathbf{m}) \\ &= \zeta^2 (1 - \|\mathbf{m}\|^2 / (1 + \|\mathbf{m}\|^2)) \\ &= \zeta^2 / (1 + \|\mathbf{m}\|^2). \end{aligned}$$

The residual  $\varepsilon_i := y_i - \langle \mathbf{w}, \mathbf{x}_i \rangle$  is independent of  $\mathbf{x}_i$  conditional on  $(\mathbf{m}, \zeta)$  by Gaussianity.  $\square$

### A.3 Law of Large Numbers for Prompt Statistics

Let  $\mathbf{X} = [\mathbf{x}_1, \dots, \mathbf{x}_L] \in \mathbb{R}^{d \times L}$  and  $\mathbf{y} = [y_1, \dots, y_L]^\top \in \mathbb{R}^L$  denote the covariate matrix and target vector, and define the context sample covariance

$$\widehat{\boldsymbol{\Lambda}} := \frac{1}{L} \mathbf{X} \mathbf{X}^\top.$$

**Lemma A.2** (Matrix LLN at fixed dimension). *Fix  $(\mathbf{m}, \zeta)$  and thus  $\boldsymbol{\Lambda} = \mathbf{I} + \mathbf{m} \mathbf{m}^\top$ . Then, almost surely as  $L \rightarrow \infty$ ,*

$$\widehat{\boldsymbol{\Lambda}} \rightarrow \boldsymbol{\Lambda}$$

*entry-wise, and hence also in operator norm. Moreover,*

$$\frac{1}{L} \mathbf{X} \mathbf{y} \rightarrow \mathbb{E}[\mathbf{x}_i y_i \mid \mathbf{m}, \zeta] = \zeta \mathbf{m}, \quad \frac{1}{L} \sum_{i=1}^L y_i^2 \rightarrow \mathbb{E}[y_i^2 \mid \mathbf{m}, \zeta] = \zeta^2.$$

*Finally, writing  $y_i = \langle \mathbf{w}, \mathbf{x}_i \rangle + \varepsilon_i$  as in Lemma A.1 and letting  $\boldsymbol{\varepsilon} = (\varepsilon_1, \dots, \varepsilon_L)^\top$ ,*

$$\frac{1}{L} \mathbf{X} \boldsymbol{\varepsilon} \rightarrow \mathbf{0} \quad \text{almost surely.}$$

*Proof.* Conditional on  $(\mathbf{m}, \zeta)$ , the pairs  $(\mathbf{x}_i, y_i)$  are i.i.d. Gaussian with finite second moments, so the stated convergences follow from the law of large numbers entrywise.  $\square$

## B Proof of Theorem 4.1

Recall the single-layer LSA predictor

$$\hat{y}_q = \text{LSA}(\mathbf{E}_X; \theta)_{d+1, L+1}, \quad \text{LSA}(\mathbf{E}_X; \theta) = \mathbf{E}_X + \mathbf{W}_{PV} \mathbf{E}_X \cdot \frac{\mathbf{E}_X^\top \mathbf{W}_{KQ} \mathbf{E}_X}{L},$$

where

$$\mathbf{E}_X = \begin{bmatrix} \mathbf{X} & \mathbf{x}_q \\ \mathbf{y}^\top & 0 \end{bmatrix} \in \mathbb{R}^{(d+1) \times (L+1)}.$$

We provide the full proof of Theorem 4.1 below.

*Proof of Theorem 4.1.* Let us write the weight matrix  $\mathbf{W}_{KQ}$  in block form

$$\mathbf{W}_{KQ} = \begin{bmatrix} \mathbf{A} & \mathbf{b}' \\ \mathbf{b}^\top & c \end{bmatrix}, \quad \mathbf{A} \in \mathbb{R}^{d \times d}, \mathbf{b}, \mathbf{b}' \in \mathbb{R}^d, c \in \mathbb{R},$$

and denote the last row of  $\mathbf{W}_{PV}$  by

$$\begin{bmatrix} \mathbf{u}^\top & v \end{bmatrix} := \mathbf{e}_{d+1}^\top \mathbf{W}_{PV}, \quad \mathbf{u} \in \mathbb{R}^d, v \in \mathbb{R}.$$

Since  $(\mathbf{E}_X)_{d+1, L_{te}+1} = 0$ , the residual term (skip-connection) in  $\text{LSA}(\mathbf{E}_X; \theta)$  does not contribute to the predictor  $\hat{y}_q$  and so

$$\hat{y}_q = \mathbf{e}_{d+1}^\top \mathbf{W}_{PV} \mathbf{E}_X \cdot \frac{\mathbf{E}_X^\top \mathbf{W}_{KQ} \mathbf{E}_X}{L_{te}} \mathbf{e}_{L_{te}+1}.$$

For  $i \in [L_{te}]$ , the  $i$ -th entry of the vector  $\mathbf{E}_X^\top \mathbf{W}_{KQ} \mathbf{E}_X \mathbf{e}_{L_{te}+1}$  is given by

$$[\mathbf{E}_X^\top \mathbf{W}_{KQ} \mathbf{E}_X \mathbf{e}_{L_{te}+1}]_i = \begin{bmatrix} \mathbf{x}_i \\ y_i \end{bmatrix}^\top \begin{bmatrix} \mathbf{A} & \mathbf{b}' \\ \mathbf{b}^\top & c \end{bmatrix} \begin{bmatrix} \mathbf{x}_q \\ 0 \end{bmatrix} = (\mathbf{x}_i^\top \mathbf{A} \mathbf{x}_q + y_i \mathbf{b}^\top \mathbf{x}_q).$$

Moreover, the  $(L_{te}+1)$ -th entry of  $\frac{1}{L_{te}} \mathbf{E}_X^\top \mathbf{W}_{KQ} \mathbf{E}_X \mathbf{e}_{L_{te}+1}$  is of order  $O(\frac{1}{L_{te}})$  and thus negligible as  $L_{te} \rightarrow \infty$ . Hence, we obtain

$$\hat{y}_q = \frac{1}{L_{te}} \sum_{i=1}^{L_{te}} (\mathbf{u}^\top \mathbf{x}_i + v y_i) (\mathbf{x}_i^\top \mathbf{A} + y_i \mathbf{b}^\top) \mathbf{x}_q + o(1). \quad (\text{B.1})$$

Conditioned on  $(\mathbf{m}, \zeta)$ , the context tokens  $\{(\mathbf{x}_i, y_i)\}_{i=1}^{L_{te}}$  are i.i.d., and  $\mathbf{x}_q$  is independent of  $\{(\mathbf{x}_i, y_i)\}_{i=1}^{L_{te}}$  with the same conditional law as  $\mathbf{x}_i$ . Applying Lemma A.2 to each empirical moment that appears when expanding (B.1) yields, almost surely (for fixed  $(\mathbf{m}, \zeta, \mathbf{x}_q)$ ),

$$\hat{y}_q \rightarrow \langle \hat{\mathbf{w}}, \mathbf{x}_q \rangle,$$

as  $L_{te} \rightarrow \infty$  where the limiting regression vector  $\hat{\mathbf{w}} = \hat{\mathbf{w}}(\mathbf{m}, \zeta) \in \mathbb{R}^d$  is

$$\hat{\mathbf{w}}(\mathbf{m}, \zeta)^\top = \mathbf{u}^\top \mathbf{\Lambda} \mathbf{A} + \left( (\mathbf{u}^\top \mathbf{m}) \mathbf{b}^\top + v \mathbf{m}^\top \mathbf{A} \right) \zeta + v \mathbf{b}^\top \zeta^2. \quad (\text{B.2})$$

We now show that  $\mathbb{P}(\hat{\mathbf{w}}(\mathbf{m}, \zeta) = \mathbf{w}(\mathbf{m}, \zeta)) = 0$ . We begin by assuming, for contradiction, that indeed  $\langle \hat{\mathbf{w}}, \mathbf{x}_q \rangle = \langle \mathbf{w}, \mathbf{x}_q \rangle$  and then examine the measure of this event. Since  $\mathbf{x}_q | (\mathbf{m}, \zeta) \sim \mathcal{N}(0, \mathbf{\Lambda})$ , we must have  $\hat{\mathbf{w}}(\mathbf{m}, \zeta) = \mathbf{w}(\mathbf{m}, \zeta)$ . Note that the Bayes vector  $\mathbf{w}$  is linear in  $\zeta$ , while, in contrast,  $\hat{\mathbf{w}}(\mathbf{m}, \zeta)$  in (B.2) is a polynomial in  $\zeta$  of degree two and so the  $\zeta^2$ -coefficient must vanish:  $v \mathbf{b} = \mathbf{0}_d$ . Similarly, since  $\mathbf{w}$  has no constant ( $\zeta^0$ ) term, we must have  $\mathbf{A}^\top \mathbf{\Lambda} \mathbf{u} = \mathbf{0}_d$ . It then follows that

$$\hat{\mathbf{w}}(\mathbf{m}, \zeta)^\top = \mathbf{m}^\top \mathbf{B} \zeta \quad (\text{B.3})$$

for the fixed matrix  $\mathbf{B} = \mathbf{u}\mathbf{b}^\top + v\mathbf{A}$ . Recalling that

$$\mathbf{w} = \frac{\zeta}{1 + \|\mathbf{m}\|^2} \mathbf{m},$$

by transposing (B.3), it follows that  $(1 + \|\mathbf{m}\|^2)^{-1}$  is an eigenvalue of  $\mathbf{B}^\top$ , equivalently of  $\mathbf{B}$ . Since  $\|\mathbf{m}\|$  is atomless while the spectrum of  $\mathbf{B}$  is finite, this cannot occur—explicitly,

$$\sup_{\mathbf{B} \in \mathbb{R}^{d \times d}} \mathbb{P} \left( \frac{1}{1 + \|\mathbf{m}\|^2} \in \sigma(\mathbf{B}) \right) = 0$$

where  $\sigma(\mathbf{B})$  denotes the spectrum of  $\mathbf{B}$ . Hence,

$$\mathbb{P}(\hat{\mathbf{w}}(\mathbf{m}, \zeta) = \mathbf{w}(\mathbf{m}, \zeta)) = 0$$

which establishes the desired result. □

## C CA Algebra and Preliminaries

This appendix collects algebraic identities for the LCA stack and the final LSA readout. These identities are used in the proofs of Theorems 6.2 and 6.3.

### C.1 LSA Readout with Frozen Parameters

Recall the (fixed) readout parameters from Section 5.1:

$$\mathbf{W}^{PV} = \begin{bmatrix} \mathbf{0}_{d \times d} & \mathbf{0}_d \\ \mathbf{0}_d^\top & 1 \end{bmatrix}, \quad \mathbf{W}^{KQ} = \begin{bmatrix} \mathbf{I}_d & \mathbf{0}_d \\ \mathbf{0}_d^\top & 0 \end{bmatrix}.$$

**Lemma C.1** (Closed-form readout). *With the above  $\mathbf{W}^{PV}$ ,  $\mathbf{W}^{KQ}$ , the single-layer LSA readout satisfies*

$$\hat{y}_q = \text{LSA}(\mathbf{E}_F)_{d+1, L+1} = \mathbf{w}^\top \left[ \frac{1}{L} \sum_{i=1}^L \mathbf{x}_i \mathbf{f}_i^\top \right] \mathbf{x}_q + \left[ \frac{1}{L} \sum_{i=1}^L \varepsilon_i \mathbf{f}_i^\top \right] \mathbf{x}_q,$$

and

$$\left[ \frac{1}{L} \sum_{i=1}^L \varepsilon_i \mathbf{f}_i^\top \right] \mathbf{x}_q \rightarrow 0$$

almost surely as  $L \rightarrow \infty$  if  $\sup_{i \geq 1} \|\mathbf{f}_i\| < \infty$ .

*Proof.* By definition,

$$\text{LSA}(\mathbf{E}_F) = \mathbf{E}_F + \mathbf{W}^{PV} \mathbf{E}_F \cdot \frac{\mathbf{E}_F^\top \mathbf{W}^{KQ} \mathbf{E}_F}{L}.$$

Since  $(\mathbf{E}_F)_{d+1,L+1} = 0$ , given the definitions of  $\mathbf{W}^{PV}$  and  $\mathbf{W}^{KQ}$ , we have

$$\begin{aligned}
\hat{y}_q &= \mathbf{e}_{d+1}^\top \mathbf{W}^{PV} \mathbf{E}_F \cdot \frac{\mathbf{E}_F^\top \mathbf{W}^{KQ} \mathbf{E}_F}{L} \mathbf{e}_{L+1} \\
&= \mathbf{e}_{d+1}^\top \frac{\mathbf{E}_F \mathbf{E}_F^\top}{L} \begin{bmatrix} \mathbf{x}_q \\ 0 \end{bmatrix} \\
&= \mathbf{e}_{d+1}^\top \frac{1}{L} \begin{bmatrix} \mathbf{F} \mathbf{F}^\top + \mathbf{x}_q \mathbf{x}_q^\top & \mathbf{F} \mathbf{y} \\ \mathbf{y}^\top \mathbf{F}^\top & \mathbf{y}^\top \mathbf{y} \end{bmatrix} \begin{bmatrix} \mathbf{x}_q \\ 0 \end{bmatrix} \\
&= \frac{\mathbf{y}^\top \mathbf{F}^\top \mathbf{x}_q}{L} \\
&= \mathbf{w}^\top \left[ \frac{1}{L} \sum_{i=1}^L \mathbf{x}_i \mathbf{f}_i^\top \right] \mathbf{x}_q + \left[ \frac{1}{L} \sum_{i=1}^L \varepsilon_i \mathbf{f}_i^\top \right] \mathbf{x}_q.
\end{aligned}$$

Hence, since  $\mathbb{E}[\varepsilon_i] = 0$  and  $\varepsilon_i \perp \mathbf{f}_i$  as  $\mathbf{F}$  depends only on  $\mathbf{X}$ , the law of large numbers yields

$$\left[ \frac{1}{L} \sum_{i=1}^L \varepsilon_i \mathbf{f}_i^\top \right] \mathbf{x}_q \rightarrow 0$$

almost surely as  $L \rightarrow \infty$ . □

Recall now that  $\mathbf{F}$  and hence  $\{\mathbf{f}_i\}_{i \geq 1}$  depend on the model depth  $T$ . From Lemma C.1, we see that if

$$\frac{1}{L} \mathbf{X} \mathbf{F}^\top \rightarrow \mathbf{I}_d$$

as  $T \rightarrow \infty$ , the asymptotic model predictor will be

$$\lim_{T \rightarrow \infty} \lim_{L \rightarrow \infty} \hat{y}_q = \langle \mathbf{w}, \mathbf{x}_q \rangle,$$

hence yielding the Bayes-optimal prediction. This will be the key step in establishing Theorems 6.2(3) and 6.3(3).

## C.2 Solving the CA Recurrence

In the one- and two-scalar simplification (Section 5.1), we take (for all layers)

$$\mathbf{W}^K = \mathbf{W}^Q = \mathbf{I}_d, \quad \mathbf{W}^S = \alpha \mathbf{I}_d, \quad \mathbf{W}^V = \beta \mathbf{I}_d,$$

where  $\alpha, \beta \in \mathbb{R}$  are scalar parameters (with the one-parameter model corresponding to  $\beta = -\alpha$ ). Layer-wise, the model then becomes, for  $t = 1, \dots, T$ ,

$$\mathbf{F}_t = \mathbf{F}_{t-1} + \alpha \mathbf{X} + \frac{\beta}{L} \mathbf{X} \mathbf{X}^\top \mathbf{F}_{t-1},$$

with  $\mathbf{F}_0 = \mathbf{0}_{d \times L}$  and  $\mathbf{F} = \mathbf{F}_T$ . Define the sample covariance  $\hat{\mathbf{\Lambda}} := \frac{1}{L} \mathbf{X} \mathbf{X}^\top$ . The following result yields a closed-form expression for the final output of the CA stack and establishes the parameter window for which one obtains the Bayes-predictor.

**Lemma C.2.** *The output of the final layer of the CA network is*

$$\mathbf{F} = \mathbf{F}_T = \alpha \sum_{k=0}^{T-1} \mathbf{M}^k \mathbf{X} \quad \text{where} \quad \mathbf{M} = \mathbf{I} + \beta \hat{\mathbf{\Lambda}}.$$

and, for  $\beta \neq 0$ ,

$$\frac{1}{L} \mathbf{X} \mathbf{F}^\top = \frac{\alpha}{\beta} \left[ (\mathbf{I} + \beta \widehat{\boldsymbol{\Lambda}})^T - \mathbf{I} \right].$$

If  $\alpha = -\beta \in (0, 2/(1 + \overline{m}))$ , then as context length  $L \rightarrow \infty$  followed by the number of layers  $T \rightarrow \infty$ , we have

$$\frac{1}{L} \mathbf{X} \mathbf{F}^\top \rightarrow \mathbf{I}.$$

almost surely.

*Proof.* We prove the first statement by induction. For the base case  $T = 1$ , we have trivially  $\mathbf{F}_1 = \alpha \mathbf{X}$  since  $\mathbf{F}_0 = \mathbf{0}_{d \times L}$ . Now, suppose  $\mathbf{F}_{T-1} = \alpha \sum_{k=0}^{T-2} \mathbf{M}^k \mathbf{X}$ . Then,

$$\begin{aligned} \mathbf{F}_T &= \mathbf{F}_{T-1} + \alpha \mathbf{X} + \beta \widehat{\boldsymbol{\Lambda}} \mathbf{F}_{T-1} \\ &= \alpha \mathbf{X} + (\mathbf{I} + \beta \widehat{\boldsymbol{\Lambda}}) \mathbf{F}_{T-1} \\ &= \alpha \mathbf{X} + \alpha \mathbf{M} \sum_{k=0}^{T-2} \mathbf{M}^k \mathbf{X} \\ &= \alpha \mathbf{X} + \alpha \sum_{k=1}^{T-1} \mathbf{M}^k \mathbf{X} = \alpha \sum_{k=0}^{T-1} \mathbf{M}^k \mathbf{X} \end{aligned}$$

which completes the induction. As  $\mathbf{M}$  is symmetric and  $\widehat{\boldsymbol{\Lambda}} = \beta^{-1}(\mathbf{M} - \mathbf{I})$ , a simple computation then yields

$$\begin{aligned} \frac{1}{L} \mathbf{X} \mathbf{F}^\top &= \alpha \widehat{\boldsymbol{\Lambda}} \sum_{k=0}^{T-1} \mathbf{M}^k = \frac{\alpha}{\beta} \sum_{k=0}^{T-1} (\mathbf{M}^{k+1} - \mathbf{M}^k) \\ &= \frac{\alpha}{\beta} (\mathbf{M}^T - \mathbf{I}) = \frac{\alpha}{\beta} \left[ (\mathbf{I} + \beta \widehat{\boldsymbol{\Lambda}})^T - \mathbf{I} \right]. \end{aligned}$$

Now, if  $\alpha = -\beta$ , we have

$$\frac{1}{L} \mathbf{X} \mathbf{F}^\top = \mathbf{I} - (\mathbf{I} - \alpha \widehat{\boldsymbol{\Lambda}})^T \rightarrow \mathbf{I} - (\mathbf{I} - \alpha \boldsymbol{\Lambda})^T$$

as  $L \rightarrow \infty$  by the Law of Large Numbers. As  $\boldsymbol{\Lambda} = \mathbf{I} + \mathbf{m} \mathbf{m}^\top$ , the eigenvalues of  $\mathbf{I} - \alpha \boldsymbol{\Lambda}$  are  $1 - \alpha$  and  $1 - \alpha(1 + \|\mathbf{m}\|^2)$ . Hence, for the choice of  $\alpha \in (0, 2/(1 + \overline{m}))$ , it follows that the operator norm  $\|\mathbf{I} - \alpha \boldsymbol{\Lambda}\| < 1$  almost surely and so  $(\mathbf{I} - \alpha \boldsymbol{\Lambda})^T \rightarrow \mathbf{0}_{d \times d}$  as  $T \rightarrow \infty$  almost surely.  $\square$

*Remark C.3.* From the proof of Lemma C.2, we see that at asymptotic context length the error away from the Bayes-optimal prediction decays geometrically in depth  $T$  so long as the model parameters satisfy  $\alpha = -\beta \in (0, 2/(1 + \overline{m}))$ . Hence, although the result concerns the behavior at infinite depth, in practice small to moderate depth networks should suffice for accurate in-context predictions. This intuition is supported by numerical experiments in Section 7.

## D Proof of Theorem 6.2

This appendix proves Theorem 6.2 for the one-parameter model, i.e. the simplified CA stack with  $\beta = -\alpha$  trained by gradient flow on the limiting population loss. Throughout, we assume Assumption 6.1:  $\|\mathbf{m}\|^2$  is almost surely bounded and has non-degenerate continuous support. Define

$$Z := 1 + \|\mathbf{m}\|^2, \quad \underline{Z} := \text{ess inf } Z, \quad \overline{Z} := \text{ess sup } Z,$$

so  $1 \leq \underline{Z} < \overline{Z} < \infty$ . We begin by determining a simplified form for the loss  $\ell(\alpha)$  and collecting some of its properties.

**Lemma D.1** (One-parameter loss). *The loss  $\ell(\alpha)$  has the form*

$$\ell(\alpha) = \mathbb{E} \left[ \frac{Z-1}{Z} (1 - \alpha Z)^{2T} \right]$$

up to the additive constant  $\mathbb{E}[1/Z]$ , where  $Z = 1 + \|\mathbf{m}\|^2$ . Moreover, the loss has the following properties:

1.  $\ell(\alpha)$  is strictly convex and coercive in the sense that

$$\lim_{|\alpha| \rightarrow \infty} \ell(\alpha) = \infty;$$

2.  $\ell(\alpha)$  has a unique minimizer which lies in  $(0, 1)$ .

*Proof.* By Lemma C.2, the model output can be written as

$$\hat{y}_q = \mathbf{w}^\top (\mathbf{I} - \mathbf{M}^T) \mathbf{x}_q + \frac{1}{L} \boldsymbol{\varepsilon}^\top \mathbf{F}^\top \mathbf{x}_q = \mathbf{w}^\top \mathbf{x}_q - \mathbf{w}^\top \mathbf{M}^T \mathbf{x}_q + \frac{1}{L} \boldsymbol{\varepsilon}^\top \mathbf{F}^\top \mathbf{x}_q.$$

where  $\mathbf{M} = \mathbf{I} - \alpha \hat{\boldsymbol{\Lambda}}$  and  $\hat{\boldsymbol{\Lambda}}$  is the sample covariance matrix with the true covariance being  $\boldsymbol{\Lambda} = \mathbf{I} + \mathbf{m} \mathbf{m}^\top$ .

We begin by conditioning on  $\boldsymbol{\Lambda}$  so that  $\mathbf{x}_i \stackrel{\text{i.i.d.}}{\sim} \mathcal{N}(0, \boldsymbol{\Lambda})$  and  $\mathbf{w} \perp \mathbf{X}, \mathbf{x}_q$ . Then, set  $\sigma^2 := \mathbb{E}[\varepsilon_i^2 | \boldsymbol{\Lambda}]$  and  $\boldsymbol{\Sigma}_w := \text{Cov}(\mathbf{w} | \boldsymbol{\Lambda})$ . Notice that

$$y_q - \hat{y}_q = \mathbf{w}^\top \mathbf{M}^T \mathbf{x}_q + \varepsilon_q - \frac{1}{L} \boldsymbol{\varepsilon}^\top \mathbf{F}^\top \mathbf{x}_q.$$

Let  $\ell(\alpha | \boldsymbol{\Lambda})$  denote the loss  $\ell(\alpha)$  where one conditions on  $\boldsymbol{\Lambda}$ . We have

$$\begin{aligned} \ell(\alpha | \boldsymbol{\Lambda}) &= \mathbb{E}[(\mathbf{w}^\top \mathbf{M}^T \mathbf{x}_q)^2 | \boldsymbol{\Lambda}] + \frac{1}{L^2} \mathbb{E}[(\boldsymbol{\varepsilon}^\top \mathbf{F}^\top \mathbf{x}_q)^2 | \boldsymbol{\Lambda}] + \mathbb{E}[\varepsilon_q^2 | \boldsymbol{\Lambda}] \\ &= \mathbb{E}[\text{tr}(\boldsymbol{\Sigma}_w \mathbf{M}^T \boldsymbol{\Lambda} \mathbf{M}^T) | \boldsymbol{\Lambda}] + \frac{1}{L^2} \mathbb{E}[\sigma^2 \text{tr}(\boldsymbol{\Lambda} \mathbf{F} \mathbf{F}^\top) | \boldsymbol{\Lambda}] + \mathbb{E}[\varepsilon_q^2 | \boldsymbol{\Lambda}] \\ &= \mathbb{E}[\text{tr}(\boldsymbol{\Sigma}_w \boldsymbol{\Lambda} \mathbf{M}^{2T}) | \boldsymbol{\Lambda}] + \frac{\alpha^2}{L} \mathbb{E}[\sigma^2 \text{tr}(\boldsymbol{\Lambda} (\sum_{k=0}^{T-1} \mathbf{M}^k (\mathbf{I} - \mathbf{M}^T))] | \boldsymbol{\Lambda}] + \mathbb{E}[\varepsilon_q^2 | \boldsymbol{\Lambda}]. \end{aligned}$$

In the first line above, the cross-terms vanish after conditioning on  $(\mathbf{m}, \zeta)$ , since  $\boldsymbol{\varepsilon}, \varepsilon_q$  are mean-zero and independent of  $\mathbf{X}, \mathbf{x}_q$ . As the training context length grows, we have

$$\ell(\alpha | \boldsymbol{\Lambda}) := \lim_{L \rightarrow \infty} \ell(\alpha | \boldsymbol{\Lambda}) = \mathbb{E}[\text{tr}(\boldsymbol{\Sigma}_w \boldsymbol{\Lambda} (\mathbf{I} - \alpha \boldsymbol{\Lambda})^{2T}) | \boldsymbol{\Lambda}] + \mathbb{E}[\varepsilon_q^2 | \boldsymbol{\Lambda}]$$

as

$$\frac{\alpha^2}{L} \mathbb{E}[\sigma^2 \text{tr}(\boldsymbol{\Lambda} (\sum_{k=0}^{T-1} \mathbf{M}^k (\mathbf{I} - \mathbf{M}^T))] | \boldsymbol{\Lambda}] \rightarrow 0 \quad \text{as } L \rightarrow \infty$$

since  $\mathbf{M} \in \mathbb{R}^{d \times d}$  and we are holding the embedding dimension  $d$  fixed. Let us write the eigen-decomposition  $\boldsymbol{\Lambda} = \mathbf{U} \boldsymbol{\Gamma} \mathbf{U}^\top$  where  $\mathbf{U}$  is an orthogonal matrix and  $\boldsymbol{\Gamma} = \text{diag}(\gamma_1, \dots, \gamma_d)$  with  $\gamma_i \geq 0$  the eigenvalues of  $\boldsymbol{\Lambda}$ . Writing  $\mathbf{V} = \mathbf{U}^\top \boldsymbol{\Sigma}_w \mathbf{U}$  which is positive semi-definite, we have

$$\ell(\alpha | \boldsymbol{\Lambda}) - \mathbb{E}[\varepsilon_q^2 | \boldsymbol{\Lambda}] = \sum_{i=1}^d v_{ii} \gamma_i (1 - \alpha \gamma_i)^{2T}.$$

where  $v_{ii} \geq 0$  for all  $i \in [d]$ . Without loss of generality, we assume that  $v_{ii}$  and  $\gamma_i$  are non-increasing in  $i \in [d]$ . Letting  $\gamma_{\max} = \gamma_1$  denote the largest eigenvalue of  $\boldsymbol{\Lambda}$ , we have that  $\gamma_{\max} = 1 + \|\mathbf{m}\|^2 = Z$  and  $\gamma_i = 1$  for  $i \geq 2$ . Since  $\mathbb{E}[\zeta^2] = 1$ , we have

$$\boldsymbol{\Sigma}_w = \frac{\mathbf{m} \mathbf{m}^\top}{(1 + \|\mathbf{m}\|^2)^2} = \frac{1}{Z} (\mathbf{I} - \boldsymbol{\Lambda}^{-1})$$

and so  $v_{11} = (Z - 1)/Z^2$  and  $v_{ii} = 0$  for  $i \geq 2$ . The conditional loss then simplifies to

$$\ell(\alpha|\mathbf{\Lambda}) = \frac{Z-1}{Z}(1-\alpha Z)^{2T} + \mathbb{E}[\varepsilon_q^2 | \mathbf{\Lambda}].$$

Moreover,

$$\mathbb{E}[\varepsilon_q^2 | \mathbf{\Lambda}] = \mathbb{E}\left[\frac{\zeta^2}{1 + \|\mathbf{m}\|^2} \mid \mathbf{\Lambda}\right] = \frac{1}{Z}.$$

Thus, up to the additive constant  $\mathbb{E}[1/Z]$ , the unconditional loss is given by

$$\ell(\alpha) = \mathbb{E}\left[\frac{Z-1}{Z}(1-\alpha Z)^{2T}\right]$$

as claimed.

1. Since  $\frac{Z-1}{Z}(1-\alpha Z)^{2T}$  is strictly convex in  $\alpha$  for  $Z > 0$  and  $\mathbb{P}(Z > 0) > 0$  by assumption 6.1, it follows that  $\ell(\alpha)$  is strictly convex. Similarly, coercivity of  $\frac{Z-1}{Z}(1-\alpha Z)^{2T}$  carries over to  $\ell(\alpha)$  by simply taking the expectation.
2. By (1),  $\ell(\alpha)$  has a unique minimizer. The first derivative of the loss is given by

$$\ell'(\alpha) = -2T\mathbb{E}[(Z-1)(1-\alpha Z)^{2T-1}].$$

Hence,

$$\text{sign}(\ell'(\alpha)) = \begin{cases} -1, & \text{if } \alpha \leq 0, \\ 1, & \text{if } \alpha \geq 1, \end{cases}$$

since  $(1-\alpha Z)^{2T-1} \leq 0$  when  $\alpha \geq 1$  because  $Z \geq 1$ . Thus, the unique root of  $\ell'(\alpha)$  is contained in  $(0, 1)$ . □

## D.1 Convergence of Gradient Flow

Given the above established properties of  $\ell(\alpha)$ , by standard dynamical systems theory results, we can derive the global convergence of gradient flow on the one-parameter loss. We include a detailed proof to initiate the unfamiliar reader.

**Lemma D.2** (One-parameter gradient flow convergence). *Suppose Assumption 6.1 holds. Then, gradient flow on  $\ell(\alpha)$  converges globally to the unique minimum of  $\ell$  whose existence is guaranteed by Lemma D.1.*

*Proof.* Let  $(\alpha_t)_{t \geq 0}$  be the gradient flow trajectory initialized at  $\alpha_0 \in \mathbb{R}$  and let  $\alpha^*$  denote the unique minimizer of  $\ell(\alpha)$ . By chain rule and the definition of gradient flow, we have

$$\frac{d}{dt}\ell(\alpha_t) = \nabla_{\alpha}\ell(\alpha_t)\dot{\alpha}_t = -\|\nabla_{\alpha}\ell(\alpha_t)\|^2 \leq 0.$$

Hence, the trajectory of the loss function  $\ell(\alpha_t)$  is decreasing and since  $\ell(\alpha) \geq 0$ , it follows that  $\ell(\alpha_t)$  converges as  $t \rightarrow \infty$ . Moreover, by coercivity of  $\ell$ ,  $\alpha_t \in \{\alpha : \ell(\alpha) \leq \ell(\alpha_0)\}$  for all  $t$  which is compact. Thus, as  $\ell \in C^\infty$ ,  $\ell'(\alpha_t)$  is uniformly continuous for all  $t \geq 0$ . Then, by Barbalat's Lemma [Slotine et al., 1991],  $\ell'(\alpha_t) \rightarrow 0$  as  $t \rightarrow \infty$ . As  $\alpha_t \in \{\alpha : \ell(\alpha) \leq \ell(\alpha_0)\}$  which is compact, moving to a convergent subsequence,  $\alpha_{t_k} \rightarrow \bar{\alpha}$  as  $k \rightarrow \infty$ . By continuity of  $\ell'$ ,  $\ell'(\alpha_{t_k}) \rightarrow \ell'(\bar{\alpha}) = 0$ . Hence,  $\bar{\alpha} = \alpha^*$  which is the unique minimizer of  $\ell$ . Hence, as every subsequence of  $(\alpha_t)_{t \geq 1}$  converges to  $\alpha^*$ , it follows that  $\alpha_t \rightarrow \alpha^*$  as  $t \rightarrow \infty$ . □

## D.2 Asymptotic Depth Behavior

Having thus far established the convergence of gradient flow at finite depth  $T$ , we now complete the proof of Theorem 6.2 with the following result which shows that as  $T \rightarrow \infty$ , we recover the optimal prediction of the model. Formally, let  $\alpha_T^*$  denote the limit of the gradient flow on the  $T$ -layer model which, from Lemma D.2, exists and coincides with the global minimum of  $\ell(\alpha)$ .

**Theorem D.3.** *Suppose Assumption 6.1 holds. Let  $\alpha_T^*$  denote the global minimum of  $\ell(\alpha)$  for the  $T$ -layer CA model which exists uniquely by Lemma D.1. Then,*

$$\lim_{T \rightarrow \infty} \alpha_T^* =: \alpha_\infty^* = \frac{2}{2 + \underline{m} + \overline{m}} = \frac{2}{\underline{Z} + \overline{Z}}.$$

Hence, the model is Bayes optimal by Lemmas C.1 and C.2.

*Proof.* Consider for  $\alpha \in [0, 1]$ , the function

$$\phi(\alpha) := \max_{z \in [\underline{Z}, \overline{Z}]} |1 - \alpha z| = \max\{|1 - \alpha \underline{Z}|, |1 - \alpha \overline{Z}|\}.$$

As the composition of a convex function with an affine function,  $z \mapsto |1 - \alpha z|$  is convex. On any interval, the maximum of a convex function occurs at the interval's endpoints and so

$$\phi(\alpha) = \max\{|1 - \alpha \underline{Z}|, |1 - \alpha \overline{Z}|\}.$$

Note that  $\phi(\alpha)$  is convex as the maximum of convex functions. The minimum of  $\phi(\alpha)$  occurs when  $|1 - \alpha \underline{Z}| = |1 - \alpha \overline{Z}|$ . Since  $\underline{Z} < \overline{Z}$ , the balancing occurs at opposite signs  $1 - \alpha \underline{Z} = -(1 - \alpha \overline{Z})$  which yields a unique minimizer

$$\alpha_\infty^* = \frac{2}{\underline{Z} + \overline{Z}}.$$

Now, let

$$f_T(\alpha) := \mathbb{E} \left[ \frac{Z-1}{Z} (1 - \alpha Z)^{2T} \right]^{1/2T}.$$

We use a shorthand  $W = \frac{Z-1}{Z}$  and  $X_\alpha = (1 - \alpha Z)$  so that

$$f_T(\alpha) = \mathbb{E}[W X_\alpha^{2T}]^{1/2T}.$$

Since  $X_\alpha \leq \phi(\alpha)$  and  $\mathbb{P}(W > 0) > 0$  by the assumption that  $\overline{Z} > \underline{Z} \geq 1$  (so  $\mathbb{E}[W] > 0$ ), we have

$$\limsup_{T \rightarrow \infty} f_T(\alpha) \leq \limsup_{T \rightarrow \infty} \mathbb{E}[W]^{1/2T} \phi(\alpha) = \phi(\alpha). \quad (\text{D.1})$$

Now, let  $(\alpha_T)_{T \geq 1}$  be a converging sequence with  $\alpha := \lim_{T \rightarrow \infty} \alpha_T$ . Notice that

$$\begin{aligned} \|X_{\alpha_T} - X_\alpha\|_\infty &= \||1 - \alpha_T Z| - |1 - \alpha Z|\|_\infty \\ &\leq \|(\alpha_T - \alpha)Z\|_\infty \\ &\leq |\alpha_T - \alpha| \overline{Z} \xrightarrow{T \rightarrow \infty} 0. \end{aligned}$$

Fixing  $\varepsilon \in (0, 1)$ , the above implies  $\|X_{\alpha_T} - X_\alpha\|_\infty \leq 1 - \varepsilon$  for  $T$  sufficiently large. The set  $S_\varepsilon := \{|X_\alpha| > \varepsilon \|X_\alpha\|_\infty\}$  satisfies  $\mathbb{P}(S_\varepsilon) > 0$  by definition of  $\|\cdot\|_\infty$ . Moreover, since  $W > 0$  a.s., there exists  $n \in \mathbb{N}$  such

that for  $A_n := \{W > 1/n\}$ , we have  $\mathbb{P}(A_n \cap S_\varepsilon) > 0$ . Putting things together, we have

$$\begin{aligned}
f_T(\alpha_T) &\geq \mathbb{E}[W X_{\alpha_T}^{2T} \mathbf{1}_{S_\varepsilon \cap A_n}]^{1/2T} \\
&\geq \left(\frac{1}{n}\right)^{1/2T} \mathbb{E}[ (|X_\alpha| - \|X_{\alpha_T} - X_\alpha\|_\infty)^{2T} \mathbf{1}_{S_\varepsilon \cap A_n} ]^{1/2T} \\
&\geq \left(\frac{1}{n}\right)^{1/2T} \mathbb{E}[(\varepsilon \|X_\alpha\|_\infty - \varepsilon + 1)^{2T} \mathbf{1}_{S_\varepsilon \cap A_n}]^{1/2T} \\
&= \left(\frac{\mathbb{P}(S_\varepsilon \cap A_n)}{n}\right)^{1/2T} (\varepsilon \|X_\alpha\|_\infty - \varepsilon + 1) \\
&\xrightarrow{T \rightarrow \infty} \varepsilon \|X_\alpha\|_\infty - \varepsilon + 1
\end{aligned}$$

Noticing that  $\phi(\alpha) = \|X_\alpha\|_\infty$ , taking  $\varepsilon \uparrow 1$ , we obtain

$$\liminf_{T \rightarrow \infty} f_T(\alpha_T) \geq \phi(\alpha). \quad (\text{D.2})$$

Now, note that  $(\alpha_T^*)_{T \geq 1} \subset [0, 1]$  by Lemma D.1(2). Therefore, we can extract a convergent subsequence  $(\alpha_{T_k}^*)_{k \geq 1}$  whose limit we denote by  $\bar{\alpha}$ . Since  $\alpha_{T_k}^*$  minimizes  $\ell$  (at depth  $T_k$ ) and hence  $f_{T_k}$ , from (D.1), we have

$$f_{T_k}(\alpha_{T_k}^*) \leq f_{T_k}(\alpha_\infty^*) \implies \limsup_{k \rightarrow \infty} f_{T_k}(\alpha_{T_k}^*) \leq \phi(\alpha_\infty^*).$$

Applying (D.2), we then have

$$\phi(\bar{\alpha}) \leq \liminf_{k \rightarrow \infty} f_{T_k}(\alpha_{T_k}^*) \leq \limsup_{k \rightarrow \infty} f_{T_k}(\alpha_{T_k}^*) \leq \phi(\alpha_\infty^*).$$

Since  $\alpha_\infty^*$  is the unique minimizer of  $\phi$ , it follows that  $\bar{\alpha} = \alpha_\infty^*$ . This completes the proof since if every convergent subsequence has the same limit, it follows that the sequence itself converges and shares this limit.  $\square$

## E Proof of Theorem 6.3

We now turn our attention to the model with the pair of learnable parameters  $(\alpha, \beta)$ . As before, we begin by determining a simplified form for the loss  $\ell(\alpha, \beta)$  and collect some properties. Recall,  $Z = 1 + \|\mathbf{m}\|^2$ .

Let

$$S := S(Z, \beta) = \frac{(1 + \beta Z)^T - 1}{\beta} \quad \text{where} \quad S(Z, 0) = \lim_{\beta \rightarrow 0} S(\beta, Z) = TZ,$$

$$W = \frac{Z - 1}{Z},$$

and

$$A(\beta) = \mathbb{E}[W S^2], \quad B(\beta) = \mathbb{E}[W S].$$

**Lemma E.1** (Two-parameter loss). *The loss  $\ell(\alpha, \beta)$  has the form*

$$\ell(\alpha, \beta) = \mathbb{E} \left[ \frac{Z - 1}{Z} \left( \frac{\alpha}{\beta} [(1 + \beta Z)^T - 1] - 1 \right)^2 \right]$$

up to the additive constant  $\mathbb{E}[1/Z]$ . Moreover, for fixed  $\beta \in \mathbb{R}$ , the loss is strongly convex in  $\alpha$ , with unique minimizer:

$$\alpha^*(\beta) := \frac{B(\beta)}{A(\beta)}.$$

*Proof.* We have

$$\begin{aligned}
\frac{\mathbf{y}^\top \mathbf{F}^\top \mathbf{x}_q}{L} &= \frac{\mathbf{w}^\top \mathbf{X} \mathbf{F}^\top \mathbf{x}_q}{L} + \frac{\boldsymbol{\varepsilon}^\top \mathbf{F}^\top \mathbf{x}_q}{L} \\
&= \frac{\alpha}{\beta} \mathbf{w}^\top (\mathbf{M}^T - \mathbf{I}) \mathbf{x}_q + \frac{\boldsymbol{\varepsilon}^\top \mathbf{F}^\top \mathbf{x}_q}{L} \\
&= -\frac{\alpha}{\beta} \mathbf{w}^\top \mathbf{x}_q + \frac{\alpha}{\beta} \mathbf{w}^\top (\mathbf{I} + \beta \hat{\boldsymbol{\Lambda}})^T \mathbf{x}_q + \frac{\boldsymbol{\varepsilon}^\top \mathbf{F}^\top \mathbf{x}_q}{L}.
\end{aligned}$$

and so

$$y_q - \hat{y}_q = \left(1 + \frac{\alpha}{\beta}\right) \mathbf{w}^\top \mathbf{x}_q - \frac{\alpha}{\beta} \mathbf{w}^\top (\mathbf{I} + \beta \hat{\boldsymbol{\Lambda}})^T \mathbf{x}_q - \frac{\boldsymbol{\varepsilon}^\top \mathbf{F}^\top \mathbf{x}_q}{L} + \varepsilon_q.$$

Taking  $L \rightarrow \infty$  so that  $\frac{\boldsymbol{\varepsilon}^\top \mathbf{F}^\top \mathbf{x}_q}{L}$  is negligible, and omitting  $\mathbb{E}[\varepsilon_q^2 | \boldsymbol{\Lambda}]$  which does not depend on  $(\alpha, \beta)$ , we have, up to the additive constant  $\mathbb{E}[1/Z]$ ,

$$\begin{aligned}
\ell(\alpha, \beta | \boldsymbol{\Lambda}) &\propto \left(1 + \frac{\alpha}{\beta}\right)^2 \mathbb{E}[(\mathbf{w}^\top \mathbf{x}_q)^2 | \boldsymbol{\Lambda}] + \left(\frac{\alpha}{\beta}\right)^2 \mathbb{E}[(\mathbf{w}^\top (\mathbf{I} + \beta \boldsymbol{\Lambda})^T \mathbf{x}_q)^2 | \boldsymbol{\Lambda}] \\
&\quad - \frac{2\alpha}{\beta} \left(1 + \frac{\alpha}{\beta}\right) \mathbb{E}[\mathbf{w}^\top \mathbf{x}_q \mathbf{w}^\top (\mathbf{I} + \beta \boldsymbol{\Lambda})^T \mathbf{x}_q | \boldsymbol{\Lambda}] \\
&= \left(1 + \frac{\alpha}{\beta}\right)^2 \text{tr}(\boldsymbol{\Sigma}_w \boldsymbol{\Lambda}) + \left(\frac{\alpha}{\beta}\right)^2 \text{tr}(\boldsymbol{\Sigma}_w \boldsymbol{\Lambda} (\mathbf{I} + \beta \boldsymbol{\Lambda})^{2T}) \\
&\quad - \frac{2\alpha}{\beta} \left(1 + \frac{\alpha}{\beta}\right) \text{tr}(\boldsymbol{\Sigma}_w \boldsymbol{\Lambda} (\mathbf{I} + \beta \boldsymbol{\Lambda})^T).
\end{aligned}$$

In the first line we used that  $\mathbb{E}[\varepsilon_i] = 0$  to get rid of cross terms and in the second, we use that  $\boldsymbol{\Sigma}_w$  commutes with  $\boldsymbol{\Lambda}$ . Recalling that

$$\boldsymbol{\Sigma}_w = \frac{\mathbf{m} \mathbf{m}^\top}{(1 + \|\mathbf{m}\|^2)^2} = \frac{1}{Z} (\mathbf{I} - \boldsymbol{\Lambda}^{-1}),$$

the loss simplifies to

$$\begin{aligned}
\ell(\alpha, \beta | \boldsymbol{\Lambda}) &= \left(1 + \frac{\alpha}{\beta}\right)^2 \frac{1}{Z} \sum_{i=1}^d (\gamma_i - 1) + \left(\frac{\alpha}{\beta}\right)^2 \frac{1}{Z} \sum_{i=1}^d (\gamma_i - 1) (1 + \beta \gamma_i)^{2T} \\
&\quad - 2 \frac{\alpha}{\beta} \left(1 + \frac{\alpha}{\beta}\right) \frac{1}{Z} \sum_{i=1}^d (\gamma_i - 1) (1 + \beta \gamma_i)^T \\
&= \left(1 + \frac{\alpha}{\beta}\right)^2 \frac{Z-1}{Z} + \left(\frac{\alpha}{\beta}\right)^2 \frac{Z-1}{Z} (1 + \beta Z)^{2T} \\
&\quad - 2 \frac{\alpha}{\beta} \left(1 + \frac{\alpha}{\beta}\right) \frac{Z-1}{Z} (1 + \beta Z)^T \\
&= \frac{Z-1}{Z} \left(\frac{\alpha}{\beta} [(1 + \beta Z)^T - 1] - 1\right)^2.
\end{aligned}$$

For the unconditional loss, one simply takes expectation:

$$\ell(\alpha, \beta) = \mathbb{E} \left[ \frac{Z-1}{Z} \left(\frac{\alpha}{\beta} [(1 + \beta Z)^T - 1] - 1\right)^2 \right].$$

Expanding the above square, we see

$$\ell(\alpha, \beta) = \alpha^2 \mathbb{E}[W S^2] - 2\alpha \mathbb{E}[W S] + \mathbb{E}[W] = \alpha^2 A(\beta) - 2\alpha B(\beta) + \mathbb{E}[W]$$

is quadratic in  $\alpha$ —hence strongly convex—and thus has a unique minimizer at  $B(\beta)/A(\beta)$ .  $\square$

In light of Lemma E.1, profiling out  $\alpha$ , we can write a reduced loss

$$F_T(\beta) := \min_{\alpha \in \mathbb{R}} \ell(\alpha, \beta) = \ell(\alpha^*(\beta), \beta) = \mathbb{E}[W] - \frac{B(\beta)^2}{A(\beta)}.$$

At this point, we notice that neither the loss  $\ell(\alpha, \beta)$  nor the reduced loss  $F_T(\beta)$  are convex. Hence, the subsequent analysis establishing the convergence of gradient flow will require a different and more involved route than in the one-parameter setup.

## E.1 Convergence of Gradient Flow

In this section, we establish that at finite depth  $T$ , gradient flow on the two-parameter loss converges under suitable initialization. We first show that, regardless of initialization, the iterates  $(\alpha_t)_{t \geq 0}$  remain bounded. Then, we show that the iterates  $(\beta_t)_{t \geq 0}$  remain bounded if one initializes  $\beta_0 \in (-2/\bar{Z}, 0)$  and  $\alpha_0 = \alpha^*(\beta_0)$ . Under this setup where the iterates  $(\alpha_t, \beta_t)_{t \geq 0}$  remain bounded, we conclude by showing they must converge as  $t \rightarrow \infty$ , hence establishing convergence of the gradient flow procedure at finite layer-depth.

We first establish some preliminary properties of the function  $A(\beta)$ .

**Lemma E.2.** *Suppose Assumption 6.1 holds. Then,*

1.  $A(\beta)$  is continuous and  $\lim_{|\beta| \rightarrow \infty} A(\beta) = +\infty$ .
2.  $A^* := \inf_{\beta \in \mathbb{R}} A(\beta) > 0$ .

*Proof.* 1. Continuity follows readily by the dominated convergence theorem which may be applied as  $Z \in [\underline{Z}, \bar{Z}]$  almost surely. Let  $z_0 \in (1, \bar{Z}]$  be such that  $\mathbb{P}(Z \geq z_0) > 0$ . Then, as  $|\beta| \rightarrow \infty$ , we have

$$S(\beta, z)^2 = \left( z \sum_{k=0}^{T-1} (1 + \beta z)^k \right)^2 \asymp z^2 (1 + \beta z)^{2T-2}$$

and so  $S(\beta, z)^2 \geq z_0^2 (1 + \beta z_0)^{2T-2}$  for  $z \geq z_0$ . Thus,

$$A(\beta) = \mathbb{E}[WS^2] \geq \mathbb{E}[W \mathbf{1}_{Z \geq z_0}] z_0^2 (1 + \beta z_0)^{2T-2} \xrightarrow{|\beta| \rightarrow \infty} \infty.$$

2. Let  $C > 0$ , then on the compact set  $[-C, C]$ , by continuity of  $A(\beta)$ , its minimum  $A_{\min} := \min_{|\beta| \leq C} A(\beta)$  is attained. Assume for contradiction that  $A_{\min} = 0$ . Then,  $S(\beta^*, Z) = 0$  almost surely on  $\{Z > 1\}$  for some  $\beta^*$ . Since  $Z$  has a continuous non-degenerate distribution, this implies that

$$\sum_{k=0}^{T-1} (1 + \beta^* z)^k = 0$$

for uncountably many values of  $z$ , which is impossible for a non-zero polynomial. Hence  $A_{\min} > 0$ . As  $\lim_{|\beta| \rightarrow \infty} A(\beta) = +\infty$ , it follows that  $A^* := \inf_{\beta \in \mathbb{R}} A(\beta) > 0$ . □

We can show that the iterates  $(\alpha_t)_{t \geq 0}$  remain bounded regardless of initialization.

**Lemma E.3.** *Suppose Assumption 6.1 holds. Then,*

$$\sup_{\beta \in \mathbb{R}} |\alpha^*(\beta)| \leq \sqrt{\frac{\mathbb{E}[W]}{A^*}} =: M^* < \infty.$$

Moreover, letting  $(\alpha_t, \beta_t)_{t \geq 0}$  be any gradient flow trajectory on  $\ell$ , we have

$$\sup_{t \geq 0} |\alpha_t| \leq M^* + \sqrt{\frac{\ell(\alpha_0, \beta_0)}{A^*}} =: M_{\alpha_0, \beta_0} < \infty.$$

*Proof.* By the Cauchy-Schwarz inequality,

$$B(\beta)^2 = \mathbb{E}[W^{1/2} \cdot W^{1/2} S(\beta)]^2 \leq \mathbb{E}[W] \mathbb{E}[W S(\beta)^2] = \mathbb{E}[W] A(\beta).$$

By Lemma E.2,

$$\sup_{\beta \in \mathbb{R}} |\alpha^*(\beta)| = \sup_{\beta \in \mathbb{R}} \frac{|B(\beta)|}{A(\beta)} \leq \sqrt{\frac{\mathbb{E}[W]}{A^*}} = M^* < \infty.$$

Now, setting  $\Delta_t = \alpha_t - \alpha^*(\beta_t)$ , notice that we may write

$$\ell(\alpha, \beta) = A(\beta) \Delta^2 + \underbrace{\mathbb{E}[W] - \frac{B(\beta)^2}{A(\beta)}}_{:=C(\beta) \geq 0}$$

where the non-negativity of  $C(\beta)$  follows from the inequality  $B(\beta)^2 \leq \mathbb{E}[W] A(\beta)$ . Recall that the loss  $\ell$  is non-increasing along gradient flow for all  $t \geq 0$  which follows from  $\frac{d}{dt} \ell(\alpha_t, \beta_t) = -\|\nabla \ell(\alpha_t, \beta_t)\|^2 \leq 0$ . Hence,  $\ell(\alpha_t, \beta_t) \leq \ell(\alpha_0, \beta_0)$  for all  $t \geq 0$  and so

$$A(\beta_t) \Delta_t^2 = \ell(\alpha_t, \beta_t) - C(\beta_t) \leq \ell(\alpha_0, \beta_0).$$

Since  $A(\beta_t) \geq A^*$  by Lemma E.2, we obtain  $\sup_{t \geq 0} |\Delta_t| \leq \sqrt{\ell(\alpha_0, \beta_0)/A^*}$  and so

$$\sup_{t \geq 0} |\alpha_t| \leq \sup_{t \geq 0} |\alpha^*(\beta_t)| + \sup_{t \geq 0} |\Delta_t| \leq M^* + \sqrt{\frac{\ell(\alpha_0, \beta_0)}{A^*}} < \infty$$

as desired.  $\square$

Now, focusing on the iterates  $(\beta_t)_{t \geq 0}$ , the following result shows that these iterates remain bounded. It is convenient to introduce the probability measure

$$d\mu = \frac{W}{\mathbb{E}[W]} d\mathbb{P}$$

so that  $\mu$  is obtained by reweighting  $d\mathbb{P}$  by  $W$  and  $\mathbb{E}_\mu[Y] = \mathbb{E}[WY]/\mathbb{E}[W]$  for a random variable  $Y$ . The following remark contains a technical device which is generic under Assumption 6.1.

*Remark E.4* (Density of  $Z$  under  $\mu$ ). Suppose that under  $\mu$ ,  $Z$  has density  $g$  with respect to the Lebesgue measure on  $[\underline{Z}, \bar{Z}]$  such that (i)  $g$  is continuous; (ii)  $g(\underline{Z}) > 0$ ; and (iii)  $g(\bar{Z}) > 0$ .

Writing

$$u_T(\beta, Z) := (1 + \beta Z)^T,$$

a short calculation shows

$$F_T(\beta) = \mathbb{E}[W] \frac{\text{Var}_\mu(u_T(\beta, Z))}{\mathbb{E}_\mu[(1 - u_T(\beta, Z))^2]} \quad (\text{E.1})$$

for any  $\beta \neq 0$  which will provide a convenient representation of the loss in subsequent proofs.

**Lemma E.5.** *Suppose Assumption 6.1 holds and the conditions of Remark E.4 are satisfied, and that one initializes gradient flow at  $\alpha_0 = \alpha^*(\beta_0)$  with  $\beta_0 \in (-2/\bar{Z}, 0)$ . Then, there exists  $T' = T'(\beta_0) \in \mathbb{N}$  such that for all  $T \geq T'$ , we have*

$$\ell(\alpha_0, \beta_0) < \min\{\ell(\alpha, -2/\bar{Z}), \ell(\alpha, 0)\}$$

for all  $\alpha \in \mathbb{R}$ . Consequently, since gradient flow is non-increasing on the loss  $\ell$ , one has  $(\beta_t)_{t \geq 0} \subset (-2/\bar{Z}, 0)$ .

*Proof.* For  $\beta = 0$ , a quick derivation reveals

$$\ell(\alpha, 0) \geq \ell(\alpha^*(0), 0) = \mathbb{E}[W] - \frac{(\mathbb{E}[WZ])^2}{\mathbb{E}[WZ^2]} =: c > 0$$

for all  $\alpha \in \mathbb{R}$  by Cauchy-Schwarz where  $c$  does not depend on  $T$ . At  $\beta = -2/\bar{Z}$ , write

$$v_T(Z) := u_T(-2/\bar{Z}, Z) = (1 - 2Z/\bar{Z})^T.$$

Since  $|v_T(Z)| \leq 1$ , we have  $\mathbb{E}_\mu[(1 - u_T(\beta, Z))^2] \leq 4$ , and hence from (E.1),

$$\ell(\alpha, -2/\bar{Z}) \geq F_T(-2/\bar{Z}) \geq \frac{\mathbb{E}[W]}{4} \text{Var}_\mu(v_T(Z))$$

for all  $\alpha \in \mathbb{R}$ . We now show that  $\text{Var}_\mu(v_T(Z)) = \Omega(1/T)$ . From Remark E.4, let  $g$  denote the continuous density of  $\mu$  on  $[\underline{Z}, \bar{Z}]$ , so that  $\mathbb{E}_\mu[h(Z)] = \int_{\underline{Z}}^{\bar{Z}} h(z)g(z) dz$  and in particular, there exist  $\delta > 0$  and  $c_1 > 0$  such that

$$g(z) \geq c_1 \quad \text{for all } z \in [\bar{Z} - \delta, \bar{Z}]. \quad (\text{E.2})$$

By a change of variables  $z = \bar{Z} - y$  for  $y \in [0, \bar{Z} - \underline{Z}]$  and taking  $T$  sufficiently large so that  $1/T \leq \delta$ , we have

$$\begin{aligned} \mathbb{E}_\mu[v_T(Z)^2] &= \int_{\underline{Z}}^{\bar{Z}} (1 - 2z/\bar{Z})^{2T} g(z) dz = \int_0^{\bar{Z}-\underline{Z}} (1 - 2y/\bar{Z})^{2T} g(\bar{Z} - y) dy \\ &\geq \int_0^{1/T} (1 - 2y/\bar{Z})^{2T} g(\bar{Z} - y) dy \geq c_1 \int_0^{1/T} (1 - 2y/\bar{Z})^{2T} dy. \end{aligned}$$

where we used (E.2) for the last inequality. For  $T$  sufficiently large and  $y \in [0, 1/T]$ , we have  $2y/\bar{Z} \leq 1/2$  and so applying the standard inequality  $1 - x \geq e^{-2x}$  for  $x \in [0, 1/2]$  yields

$$\mathbb{E}_\mu[v_T(Z)^2] \geq c_1 \int_0^{1/T} \exp\left(-\frac{8Ty}{\bar{Z}}\right) dy \geq c_1 \int_0^{1/T} \exp\left(-\frac{8}{\bar{Z}}\right) dy = \Omega(1/T).$$

We now turn our attention to  $\mathbb{E}_\mu[v_T(Z)]^2$ . Since  $g$  is continuous on  $[\underline{Z}, \bar{Z}]$ , let  $c_2$  be an upper bound on  $g$  and assume without loss of generality that  $\bar{Z}/2 \leq \bar{Z} - \underline{Z}$ . Using the inequality  $1 - x \leq e^{-x}$  for  $x \in [0, 1]$  and  $|1 - 2y/\bar{Z}| =: \bar{\rho} < 1$  for all  $y \in [\bar{Z}/2, \bar{Z} - \underline{Z}]$ , we have

$$\begin{aligned} \mathbb{E}_\mu[|v_T(Z)|] &= \int_{\underline{Z}}^{\bar{Z}} |1 - 2z/\bar{Z}|^T g(z) dz = \int_0^{\bar{Z}-\underline{Z}} |1 - 2y/\bar{Z}|^T g(\bar{Z} - y) dy \\ &\leq c_2 \int_0^{\bar{Z}/2} |1 - 2y/\bar{Z}|^T dy + c_2 \int_{\bar{Z}/2}^{\bar{Z}-\underline{Z}} |1 - 2y/\bar{Z}|^T dy \\ &\leq c_2 \int_0^{\bar{Z}/2} \exp(-2Ty/\bar{Z}) dy + c_2 \int_{\bar{Z}/2}^{\bar{Z}-\underline{Z}} \bar{\rho}^T dy \\ &\leq c_2 \left( \int_0^\infty \exp(-2Ty/\bar{Z}) dy + (\bar{Z} - \underline{Z})\bar{\rho}^T \right) \\ &\leq c_2 \left( \frac{\bar{Z}}{2T} + (\bar{Z} - \underline{Z})\bar{\rho}^T \right) = O(1/T). \end{aligned}$$

By Jensen's inequality, we have  $\mathbb{E}_\mu[v_T(Z)]^2 = O(1/T^2)$  and so  $\text{Var}_\mu(v_T(Z)) = \Omega(1/T)$ . Hence, for all  $\alpha \in \mathbb{R}$ ,

$$\ell(\alpha, -2/\bar{Z}) = \Omega(1/T) \quad (\text{E.3})$$

---

<sup>2</sup>If this is not the case, the analysis below is simplified.

for all  $T$  large. Finally, note that for the fixed initialization  $\beta_0 \in (-2/\bar{Z}, 0)$ , we have

$$|u_T(\beta_0, Z)| \leq \rho_{\beta_0}^T \quad \text{for some } \rho_{\beta_0} \in (0, 1)$$

almost surely. Hence, there exists  $\bar{T}$  such that  $\mathbb{E}_\mu[(1 - u_T(\beta_0, Z))^2] \geq C > 0$  (e.g.  $C = 1/2$ ) for all  $T \geq \bar{T}$ , and so

$$F_T(\beta_0) \leq \frac{\mathbb{E}[W]\text{Var}_\mu(u_T(\beta_0, Z))}{C} \leq \frac{\mathbb{E}[W]\mathbb{E}_\mu[u_T(\beta_0, Z)^2]}{C} \leq \frac{\mathbb{E}[W]}{C}\rho_{\beta_0}^{2T} = O(\rho_{\beta_0}^{2T}).$$

Since  $\alpha_0 = \alpha^*(\beta_0)$ , we have

$$\ell(\alpha_0, \beta_0) = F_T(\beta_0) = O(\rho_{\beta_0}^{2T}).$$

Combining this with (E.3) and the lower bound  $\ell(\alpha, 0) \geq c > 0$ , it follows that there exists  $T' = T'(\beta_0)$  such that for all  $T \geq T'$ ,

$$\ell(\alpha_0, \beta_0) < \min\{\ell(\alpha, -2/\bar{Z}), \ell(\alpha, 0)\} \quad \forall \alpha \in \mathbb{R}.$$

The final claim follows because gradient flow is non-increasing on  $\ell$ .  $\square$

**Theorem E.6.** *Suppose Assumption 6.1 holds and the conditions of Remark E.4 are satisfied, and that one initializes gradient flow at  $\alpha_0 = \alpha^*(\beta_0)$  with  $\beta_0 \in (-2/\bar{Z}, 0)$ . Then, gradient flow on  $\ell(\alpha, \beta)$  converges with*

$$\beta_T^* := \lim_{t \rightarrow \infty} \beta_{t,T} \in (-2/\bar{Z}, 0)$$

and

$$\alpha_T^* := \lim_{t \rightarrow \infty} \alpha_{t,T} = \alpha^*(\beta_T^*).$$

*Proof.* By Lemma E.5, since gradient flow is non-increasing on  $\ell(\alpha, \beta)$ , it follows that  $\beta_t \in (-2/\bar{Z}, 0)$  for all  $t \geq 0$ . Moreover, from Lemma E.3, we know that  $\alpha_t$  remains bounded and so the gradient flow trajectory  $(\alpha_t, \beta_t)_{t \geq 0}$  is bounded. Since  $\ell$  is real-analytic on the open set  $\mathbb{R} \times (-2/\bar{Z}, 0)$ , the bounded trajectory  $(\alpha_t, \beta_t)_{t \geq 0}$  converges to a single critical point by the Lojasiewicz gradient inequality. Clearly,  $\alpha_T^* = \alpha^*(\beta_T^*)$  and since  $\beta_t \in (-2/\bar{Z}, 0)$  for all  $t \geq 0$ , it follows that  $\beta_T^* \in [-2/\bar{Z}, 0]$ . Moreover, by continuity of the loss  $\ell$  in  $(\alpha, \beta)$  and Lemma E.5 which shows  $\ell(\alpha_0, \beta_0) < \min\{\ell(\alpha, -2/\bar{Z}), \ell(\alpha, 0)\}$ ,  $\beta_T^* \notin \{-2/\bar{Z}, 0\}$  as if this were the case then necessarily, for  $t$  sufficiently large one would have  $\ell(\alpha_t, \beta_t) > \ell(\alpha_0, \beta_0)$ —a contradiction. Hence,  $\beta_T^*$  lies in the open interval  $(-2/\bar{Z}, 0)$ .  $\square$

## E.2 Asymptotic Depth Behavior

Having established in the previous subsection that gradient flow converges to a stationary point at any fixed depth  $T$ , we now study how these stationary points behave as the depth  $T \rightarrow \infty$ . Our goal is to understand the asymptotic depth behavior of the limits of gradient flow and to show that, as in the one-parameter case, the limiting predictor is Bayes optimal. To make explicit the dependence on depth, let  $\ell^{(T)}$  denote the loss  $\ell$  where the CA model is at depth  $T$ .

In the two-parameter setting, the loss is not jointly convex, so we cannot identify the gradient-flow limit  $(\alpha_T^*, \beta_T^*)$  as a global minimizer of  $\ell$ . However, what is guaranteed is that

$$(\alpha_T^*, \beta_T^*) \text{ is a stationary point of } \ell^{(T)} \quad \text{and} \quad \alpha_T^* = \alpha^*(\beta_T^*),$$

so in particular

$$F_T'(\beta_T^*) = 0.$$

Thus, the large-depth behavior of the gradient-flow limits is governed by the stationary points of the one-dimensional function  $\beta \mapsto F_T(\beta)$ . It will be convenient to work with a logarithmically rescaled version of  $F_T$ :

$$G_T(\beta) := \frac{1}{2T} \log \left( \frac{F_T(\beta)}{\mathbb{E}[W]} \right).$$

The function  $G_T$  is well-defined and smooth as  $F_T > 0$ . Moreover,  $G_T$  is a strictly monotone transform of  $F_T$  so  $F'_T(\beta_T^*) = 0$  if and only if  $G'_T(\beta_T^*) = 0$ . Our task is therefore to understand the asymptotic behavior of  $G_T$  and  $G'_T$  as  $T \rightarrow \infty$ , and to show that stationary points of  $F_T$  (and  $G_T$ ) concentrate near a single value of  $\beta$ .

**Lemma E.7.** *Suppose Assumption 6.1 holds and the conditions of Remark E.4 are satisfied, and fix any compact interval  $K \subset I \setminus \{-\alpha^*\}$ , where  $I := (-2/\bar{Z}, 0)$ ,  $\alpha^* := 2/(\underline{Z} + \bar{Z})$ . For each  $T \in \mathbb{N}$  and  $\beta \in K$  define the probability measure*

$$d\nu_{T,\beta}(z) := \frac{|1 + \beta z|^{2T}}{\int |1 + \beta s|^{2T} d\mu(s)} d\mu(z).$$

Then the following hold uniformly for  $\beta \in K$  as  $T \rightarrow \infty$ :

1. The reduced loss  $F_T(\beta)$  satisfies

$$F_T(\beta)^{1/(2T)} \longrightarrow \phi(\beta),$$

where

$$\phi(\beta) = \max\{|1 + \beta \underline{Z}|, |1 + \beta \bar{Z}|\}.$$

2. Let  $z^*(\beta) \in \{\underline{Z}, \bar{Z}\}$  denote the unique endpoint at which  $\phi(\beta) = |1 + \beta z^*(\beta)|$  is attained. Then  $\nu_{T,\beta}$  converges weakly to the point mass at the active endpoint.

*Proof.* We begin from the variance representation:

$$F_T(\beta) = \mathbb{E}[W] \frac{\text{Var}_\mu(u_T(\beta, Z))}{\mathbb{E}_\mu[(1 - u_T(\beta, Z))^2]}.$$

We analyze numerator and denominator separately. For the denominator, for any  $\beta \in K$  and  $z \in [\underline{Z}, \bar{Z}]$  we have

$$|1 + \beta z| \leq \phi(\beta) \leq \phi_K := \sup_{\beta \in K} \phi(\beta) < 1,$$

where  $\phi_K < 1$  by continuity of  $\phi$  and compactness of  $K$ . Thus,

$$|u_T(\beta, Z)| = |1 + \beta Z|^T \leq \phi_K^T$$

almost surely and therefore

$$\mathbb{E}_\mu[(1 - u_T(\beta, Z))^2] = 1 - 2\mathbb{E}_\mu[u_T(\beta, Z)] + \mathbb{E}_\mu[u_T(\beta, Z)^2],$$

with

$$|\mathbb{E}_\mu[u_T(\beta, Z)]| \leq \phi_K^T, \quad \mathbb{E}_\mu[u_T(\beta, Z)^2] \leq \phi_K^{2T}.$$

Hence

$$\mathbb{E}_\mu[(1 - u_T(\beta, Z))^2] \in [1 - 2\phi_K^T, 1 + \phi_K^{2T}] \xrightarrow{T \rightarrow \infty} 1$$

uniformly in  $\beta \in K$ . In particular, for all sufficiently large  $T$ , we have

$$\frac{1}{2} \leq \mathbb{E}_\mu[(1 - u_T(\beta, Z))^2] \leq 2, \quad \forall \beta \in K. \tag{E.4}$$

Now, for an upper bound on the numerator, we have

$$\text{Var}_\mu(u_T(\beta, Z)) \leq \mathbb{E}_\mu[u_T(\beta, Z)^2] = \int |1 + \beta z|^{2T} d\mu(z) \leq \phi(\beta)^{2T}. \quad (\text{E.5})$$

Now, for a lower bound on the numerator, note that for any random variable  $X$  and measurable event  $A$ , the law of total variance shows:

$$\text{Var}_\mu(X) \geq \mu(A)\mu(A^c) (\mathbb{E}[X | A] - \mathbb{E}[X | A^c])^2. \quad (\text{E.6})$$

Now, for fixed  $\beta \in K$ , we define

$$X_T(\beta) := u_T(\beta, Z) = (1 + \beta Z)^T.$$

Since the conditions of Remark E.4 hold and  $K$  is compact, there exist constants  $\varepsilon > 0$  and  $c > 0$  such that, for every  $\beta \in K$ ,

- if  $z^*(\beta) = \bar{Z}$ , then  $A_\beta := [\bar{Z} - \varepsilon, \bar{Z}]$  satisfies  $\mu(A_\beta) \geq c$ ;
- if  $z^*(\beta) = \underline{Z}$ , then  $A_\beta := [\underline{Z}, \underline{Z} + \varepsilon]$  satisfies  $\mu(A_\beta) \geq c$ .

Without loss of generality, by continuity of the map  $(\beta, z) \mapsto |1 + \beta z|$  on the compact set  $K \times [\underline{Z}, \bar{Z}]$ , we may also choose  $\varepsilon$  small enough so that there exists  $\delta \in (0, 1 - \phi_K)$  and  $\eta > 0$  with

$$|1 + \beta z| \geq \phi(\beta) - \delta \quad \text{for all } z \in A_\beta, \beta \in K, \quad (\text{E.7})$$

$$|1 + \beta z| \leq \phi(\beta) - \eta \quad \text{for all } z \in A_\beta^c, \beta \in K. \quad (\text{E.8})$$

Moreover, shrinking  $\varepsilon$  if necessary, we may assume that there exists  $\sigma \in \{-1, 1\}$  such that

$$\sigma(1 + \beta z) \geq 0 \quad \text{for all } z \in A_\beta, \beta \in K. \quad (\text{E.9})$$

Indeed, since  $K \subset I \setminus \{-\alpha^*\}$ , the active endpoint is unique for every  $\beta \in K$ , and by compactness of  $K$  the distance from  $K$  to  $-\alpha^*$  is strictly positive; this gives a uniform gap from zero for  $1 + \beta z$  on the corresponding endpoint neighborhood  $A_\beta$ .

From (E.7)–(E.8), we have  $|X_T(\beta)| \geq (\phi(\beta) - \delta)^T$  on  $A_\beta$  while  $|X_T(\beta)| \leq (\phi(\beta) - \eta)^T$  on  $A_\beta^c$ . By (E.9),  $X_T(\beta)$  has constant sign on  $A_\beta$ , and therefore

$$|\mathbb{E}[X_T(\beta) | A_\beta]| = \mathbb{E}[|X_T(\beta)| | A_\beta] \geq (\phi(\beta) - \delta)^T.$$

Also,

$$|\mathbb{E}[X_T(\beta) | A_\beta^c]| \leq (\phi(\beta) - \eta)^T.$$

Further, for all sufficiently large  $T$  we have  $(\phi(\beta) - \eta)^T \leq \frac{1}{2}(\phi(\beta) - \delta)^T$ , and so

$$|\mathbb{E}[X_T(\beta) | A_\beta] - \mathbb{E}[X_T(\beta) | A_\beta^c]| \geq (\phi(\beta) - \delta)^T - (\phi(\beta) - \eta)^T \geq \frac{1}{2}(\phi(\beta) - \delta)^T.$$

Applying the inequality (E.6) with  $X = X_T(\beta)$  and  $A = A_\beta$ , we obtain

$$\text{Var}_\mu(u_T(\beta, Z)) \geq \mu(A_\beta)\mu(A_\beta^c) (\mathbb{E}[X_T(\beta) | A_\beta] - \mathbb{E}[X_T(\beta) | A_\beta^c])^2 \geq C_1(\phi(\beta) - \delta)^{2T},$$

for all  $\beta \in K$  and all sufficiently large  $T$ , where  $C_1 := \frac{1}{4}c(1 - c) > 0$  is independent of  $\beta$ . Combining this with the upper bound (E.5), we have, for all large  $T$  and all  $\beta \in K$ ,

$$C_1(\phi(\beta) - \delta)^{2T} \leq \text{Var}_\mu(u_T(\beta, Z)) \leq \phi(\beta)^{2T}. \quad (\text{E.10})$$

Putting everything together, using (E.4) and (E.10), we obtain

$$\frac{1}{2}\mathbb{E}[W]\text{Var}_\mu(u_T(\beta, Z)) \leq F_T(\beta) \leq 2\mathbb{E}[W]\text{Var}_\mu(u_T(\beta, Z))$$

for all large  $T$  and all  $\beta \in K$ . Hence, for such  $T$ ,

$$\left(\frac{1}{2}\mathbb{E}[W]C_1\right)^{1/(2T)}(\phi(\beta) - \delta) \leq F_T(\beta)^{1/(2T)} \leq (2\mathbb{E}[W])^{1/(2T)}\phi(\beta).$$

Letting  $T \rightarrow \infty$ , we have

$$\phi(\beta) - \delta \leq \liminf_{T \rightarrow \infty} F_T(\beta)^{1/(2T)} \leq \limsup_{T \rightarrow \infty} F_T(\beta)^{1/(2T)} \leq \phi(\beta)$$

and, since  $\delta > 0$  was arbitrary, we obtain the desired uniform convergence over  $K$ .

We now turn to proving the second statement of the lemma. Fix a bounded, continuous function  $f : [\underline{Z}, \bar{Z}] \rightarrow \mathbb{R}$ . By definition of  $\nu_{T,\beta}$ ,

$$\int f(z) d\nu_{T,\beta}(z) = \frac{\int f(z) |1 + \beta z|^{2T} d\mu(z)}{\int |1 + \beta s|^{2T} d\mu(s)}. \quad (\text{E.11})$$

We will show that the right-hand side of (E.11) converges to  $f(z^*(\beta))$  uniformly in  $\beta \in K$ . Split both the numerator and denominator into contributions from  $A_\beta$  and  $A_\beta^c$ . From (E.7)–(E.8) we have

$$\int_{A_\beta} |1 + \beta z|^{2T} d\mu(z) \geq \mu(A_\beta)(\phi(\beta) - \delta)^{2T} \geq c(\phi(\beta) - \delta)^{2T}$$

and

$$\int_{A_\beta^c} |1 + \beta z|^{2T} d\mu(z) \leq (\phi(\beta) - \eta)^{2T}.$$

Thus,

$$\frac{\int_{A_\beta^c} |1 + \beta z|^{2T} d\mu(z)}{\int_{A_\beta} |1 + \beta z|^{2T} d\mu(z)} \leq \frac{(\phi(\beta) - \eta)^{2T}}{c(\phi(\beta) - \delta)^{2T}} \xrightarrow{T \rightarrow \infty} 0,$$

uniformly over  $\beta \in K$ . Therefore, the contribution of  $A_\beta^c$  to both the numerator and denominator in (E.11) is negligible. More precisely, write the numerator  $N_T(\beta)$  and denominator  $D_T(\beta)$  as

$$N_T(\beta) = \int f(z) |1 + \beta z|^{2T} d\mu(z) = N_T^{(A)}(\beta) + N_T^{(A^c)}(\beta),$$

$$D_T(\beta) = \int |1 + \beta z|^{2T} d\mu(z) = D_T^{(A)}(\beta) + D_T^{(A^c)}(\beta),$$

where the superscripts denote integration over  $A_\beta$  and  $A_\beta^c$  respectively. By boundedness of  $f$  and the previous estimates, we have

$$\frac{|N_T^{(A^c)}(\beta)|}{D_T^{(A)}(\beta)} \leq \|f\|_\infty \frac{(\phi(\beta) - \eta)^{2T}}{c(\phi(\beta) - \delta)^{2T}} \xrightarrow{T \rightarrow \infty} 0,$$

and

$$\frac{D_T^{(A^c)}(\beta)}{D_T^{(A)}(\beta)} \xrightarrow{T \rightarrow \infty} 0,$$

uniformly over  $\beta \in K$ . Hence,

$$\int f \, d\nu_{T,\beta} = \frac{N_T^{(A)}(\beta)}{D_T^{(A)}(\beta)} + o(1),$$

where  $o(1) \rightarrow 0$  uniformly in  $\beta \in K$ . Now, we restrict attention to the conditional probability measure on  $A_\beta$  with density proportional to  $|1 + \beta z|^{2T} \, d\mu(z)$ . On  $A_\beta$ , the function  $z \mapsto |1 + \beta z|$  attains its unique maximum at  $z^*(\beta)$ , since  $K \subset I \setminus \{-\alpha^*\}$  ensures that the active endpoint is unique, and the interval  $A_\beta$  can be made arbitrarily small by taking  $\varepsilon \downarrow 0$ . Since  $f$  is uniformly continuous on the compact set  $[\underline{Z}, \overline{Z}]$ , for any  $\varepsilon > 0$  we can shrink  $\varepsilon > 0$  (uniformly in  $\beta \in K$ ) so that

$$|f(z) - f(z^*(\beta))| < \varepsilon \quad \forall z \in A_\beta, \beta \in K.$$

Then,

$$\left| \frac{N_T^{(A)}(\beta)}{D_T^{(A)}(\beta)} - f(z^*(\beta)) \right| \leq \sup_{z \in A_\beta} |f(z) - f(z^*(\beta))| < \varepsilon,$$

because  $N_T^{(A)}(\beta)/D_T^{(A)}(\beta)$  is merely the expectation of  $f(Z)$  under the normalized weights  $|1 + \beta Z|^{2T} \mathbf{1}_{A_\beta} \, d\mu$ , where  $\mathbf{1}_{A_\beta}$  denotes the indicator of the set  $A_\beta$ . Combining this with the negligible contribution of  $A_\beta^c$ , we conclude that

$$\int f(z) \, d\nu_{T,\beta}(z) \longrightarrow f(z^*(\beta))$$

uniformly over  $\beta \in K$ . Since this holds for every bounded continuous  $f$ , we have  $\nu_{T,\beta} \rightarrow \delta_{z^*(\beta)}$ <sup>3</sup> weakly, uniformly over  $\beta \in K$ .  $\square$

The above result will be utilized in proving the following lemma establishing the uniform convergence of the derivatives of  $G_T$  over a compact interval omitting the point  $-\alpha^*$ . This will then yield a contradiction as the limiting derivative is strictly nonzero away from  $-\alpha^*$ . As a quick reminder from Appendix D, we defined

$$\alpha^* = \frac{2}{\underline{Z} + \overline{Z}}.$$

**Lemma E.8** (Asymptotics of the derivative). *Suppose Assumption 6.1 holds and the conditions of Remark E.4 are satisfied. Fix a compact interval  $K \subset I \setminus \{-\alpha^*\}$ , where  $I := (-2/\overline{Z}, 0)$ . Then:*

1. *The derivatives  $G'_T(\beta)$  converge uniformly on  $K$  to the derivative of  $\log \phi(\beta)$ :*

$$G'_T(\beta) \longrightarrow \frac{d}{d\beta} \log \phi(\beta)$$

*uniformly for  $\beta \in K$  as  $T \rightarrow \infty$ .*

2. *In particular, since  $-\alpha^* \notin K$ , there exist constants  $T_K < \infty$  and  $c_K > 0$  such that*

$$|G'_T(\beta)| \geq c_K > 0, \quad \forall \beta \in K, T \geq T_K.$$

*Proof.* We begin by writing

$$F_T(\beta) = \mathbb{E}[W] \frac{V_T(\beta)}{D_T(\beta)}, \quad V_T(\beta) := \text{Var}_\mu(u_T(\beta, Z)), \quad D_T(\beta) := \mathbb{E}_\mu[(1 - u_T(\beta, Z))^2].$$

Thus,

$$G_T(\beta) = \frac{1}{2T} (\log V_T(\beta) - \log D_T(\beta))$$

---

<sup>3</sup>By standard convention,  $\delta$  denotes a point-mass (Dirac measure).

and so

$$G'_T(\beta) = \frac{1}{2T} \frac{V'_T(\beta)}{V_T(\beta)} - \frac{1}{2T} \frac{D'_T(\beta)}{D_T(\beta)}. \quad (\text{E.12})$$

We analyze the two terms in (E.12) separately starting with the denominator term. For  $\beta \in K$  and  $z \in [\underline{Z}, \overline{Z}]$ , we have  $|1 + \beta z| \leq \phi_K < 1$ , thus

$$|u_T(\beta, z)| = |1 + \beta z|^T \leq \phi_K^T.$$

From the proof of Lemma E.7 we know that  $D_T(\beta) \rightarrow 1$  as  $T \rightarrow \infty$  uniformly in  $\beta \in K$ . Differentiating under the integral sign, we have

$$D'_T(\beta) = \mathbb{E}_\mu [2(1 - u_T)(-u'_T)],$$

where

$$u'_T(\beta, z) := \frac{d}{d\beta} u_T(\beta, z) = Tz(1 + \beta z)^{T-1}.$$

Therefore,

$$|D'_T(\beta)| \leq 2\mathbb{E}_\mu (|1 - u_T||u'_T|) \leq 4T\overline{Z}\phi_K^{T-1}$$

since  $|1 - u_T| \leq 1 + |u_T| \leq 2$  for large  $T$ . Consequently, for some constant  $C > 0$ ,

$$\left| \frac{1}{2T} \frac{D'_T(\beta)}{D_T(\beta)} \right| \leq C\phi_K^{T-1} \xrightarrow{T \rightarrow \infty} 0,$$

uniformly in  $\beta \in K$ , which shows that the second term in (E.12) is  $o(1)$  uniformly on  $K$ . The prior differentiation under the integral sign was justified by dominated convergence:  $|(1 - u_T)(-u'_T)| \leq 2T\overline{Z}\phi_K^{T-1}$  which is integrable w.r.t.  $\mu$  and independent of  $z$ , and for each fixed  $z$  the integrand is  $C^1$  in  $\beta$ .

We now turn to the numerator term of (E.12):  $\frac{1}{2T} \frac{V'_T(\beta)}{V_T(\beta)}$ . Since  $V_T(\beta) = \mathbb{E}_\mu[u_T^2] - \mathbb{E}_\mu[u_T]^2$  with  $u_T := u_T(\beta, Z)$ , differentiating, we obtain

$$V'_T(\beta) = \frac{d}{d\beta} \mathbb{E}_\mu[u_T^2] - 2\mathbb{E}_\mu[u_T] \frac{d}{d\beta} \mathbb{E}_\mu[u_T].$$

As above,

$$\left| \frac{d}{d\beta} \mathbb{E}_\mu[u_T] \right| \leq T\overline{Z}\phi_K^{T-1}, \quad \left| \frac{d}{d\beta} \mathbb{E}_\mu[u_T^2] \right| \leq 2T\overline{Z}\phi_K^{2T-1},$$

uniformly over  $\beta \in K$ . By (E.4) and (E.10) from Lemma E.7, we have  $V_T(\beta) \asymp \phi(\beta)^{2T}$  uniformly on  $K$ ; in particular, there exist constants  $0 < c_1 \leq c_2 < \infty$  such that

$$c_1\phi(\beta)^{2T} \leq V_T(\beta) \leq c_2\phi(\beta)^{2T} \quad \forall \beta \in K$$

for all  $T$  sufficiently large. Hence, the contribution from the term  $-2\mathbb{E}_\mu[u_T] \frac{d}{d\beta} \mathbb{E}_\mu[u_T]$  to the ratio  $\frac{1}{2T} \frac{V'_T(\beta)}{V_T(\beta)}$  can be bounded as

$$\left| \frac{1}{2T} \frac{-2\mathbb{E}_\mu[u_T] \frac{d}{d\beta} \mathbb{E}_\mu[u_T]}{V_T(\beta)} \right| \leq C'\phi_K^{T-1} \xrightarrow{T \rightarrow \infty} 0,$$

uniformly over  $\beta \in K$ , for some constant  $C' > 0$ . Thus, the main contribution to  $\frac{1}{2T} \frac{V'_T(\beta)}{V_T(\beta)}$  comes from  $\mathbb{E}_\mu[u_T^2]$ :

$$\frac{1}{2T} \frac{V'_T(\beta)}{V_T(\beta)} = \frac{1}{2T} \frac{\frac{d}{d\beta} \mathbb{E}_\mu[u_T(\beta, Z)^2]}{\mathbb{E}_\mu[u_T(\beta, Z)^2]} + o(1), \quad (\text{E.13})$$

uniformly over  $\beta \in K$ . Now

$$\mathbb{E}_\mu[u_T(\beta, Z)^2] = \int (1 + \beta z)^{2T} d\mu(z) \implies \frac{d}{d\beta} \mathbb{E}_\mu[u_T(\beta, Z)^2] = \int 2Tz(1 + \beta z)^{2T-1} d\mu(z).$$

and therefore

$$\frac{1}{2T} \frac{\frac{d}{d\beta} \mathbb{E}_\mu[u_T(\beta, Z)^2]}{\mathbb{E}_\mu[u_T(\beta, Z)^2]} = \frac{\int z(1 + \beta z)^{2T-1} d\mu(z)}{\int (1 + \beta z)^{2T} d\mu(z)} = \int \frac{z}{1 + \beta z} d\nu_{T,\beta}(z)$$

where  $\nu_{T,\beta}$  is precisely the probability measure from Lemma E.7(2). Combining with (E.13) and the negligibility of the denominator term, we obtain

$$G'_T(\beta) = \int \frac{z}{1 + \beta z} d\nu_{T,\beta}(z) + o(1), \quad (\text{E.14})$$

where  $o(1) \rightarrow 0$  uniformly over  $\beta \in K$ .

By Lemma E.7(2), for each fixed  $\beta \in K$  the measures  $\nu_{T,\beta}$  converge weakly to  $\delta_{z^*(\beta)}$ , where  $z^*(\beta) \in \{\underline{Z}, \overline{Z}\}$  is the endpoint at which  $\phi(\beta)$  is attained and this convergence is uniform in  $\beta \in K$ . Since the function  $(\beta, z) \mapsto \frac{z}{1 + \beta z}$  is continuous on  $K \times [\underline{Z}, \overline{Z}]$ , by uniform weak convergence,

$$\int \frac{z}{1 + \beta z} d\nu_{T,\beta}(z) \longrightarrow \frac{z^*(\beta)}{1 + \beta z^*(\beta)},$$

uniformly over  $\beta \in K$ . Together with (E.14), this yields

$$G'_T(\beta) \longrightarrow \frac{z^*(\beta)}{1 + \beta z^*(\beta)}$$

uniformly over  $\beta \in K$ . Now, on any compact  $K \subset I$  that does not contain  $-\alpha^*$ , the active endpoint  $z^*(\beta)$  is constant (always  $\underline{Z}$  or always  $\overline{Z}$ ), and the sign of  $1 + \beta z^*(\beta)$  is fixed. Therefore,

$$\frac{d}{d\beta} \log \phi(\beta) = \frac{d}{d\beta} \log |1 + \beta z^*(\beta)| = \frac{z^*(\beta)}{1 + \beta z^*(\beta)}.$$

and so  $G'_T(\beta) \longrightarrow \frac{d}{d\beta} \log \phi(\beta)$  as  $T \rightarrow \infty$  uniformly over  $\beta \in K$ , which proves part (1).

We can now wrap up the proof by establishing the second statement of the lemma. Note that the function  $\phi$  is smooth on  $I \setminus \{-\alpha^*\}$  and  $-\alpha^*$  is the unique minimizer of  $\phi$ . Hence  $\frac{d}{d\beta} \log \phi(\beta)$  is continuous and nonzero on  $K$ , and therefore there exists  $c_K > 0$  such that

$$\left| \frac{d}{d\beta} \log \phi(\beta) \right| \geq 2c_K$$

for all  $\beta \in K$ . By uniform convergence of  $G'_T$  to  $\frac{d}{d\beta} \log \phi(\beta)$  on  $K$ , we may choose  $T_K$  large enough so that

$$|G'_T(\beta)| \geq c_K$$

for all  $\beta \in K$  when  $T \geq T_K$ . This proves part (2) and completes the proof.  $\square$

The full result of Theorem 6.3 will now follow by a simple proof by contradiction by extracting a subsequence  $(\beta_{T_k}^*)_{k \geq 1}$  converging in the interior of the interval. The culmination of this section is now provided in the next result.

**Theorem E.9.** *Suppose the assumptions of Theorem E.6 hold. Let  $(\alpha_T^*, \beta_T^*)$  denote the limit of gradient flow on the two-parameter,  $T$ -layer, CA model whose existence is guaranteed by Theorem E.6. Moreover, assume that  $\lim_{T \rightarrow \infty} \beta_T^* \notin \{-2/\overline{Z}, 0\}$ . Then,*

$$\lim_{T \rightarrow \infty} \alpha_T^* = \alpha^* = \frac{2}{\underline{Z} + \overline{Z}}.$$

and

$$\lim_{T \rightarrow \infty} \beta_T^* = -\alpha^*.$$

Hence, the model is Bayes optimal by Lemmas C.1 and C.2.

*Proof.* We assume for contradiction that  $\lim_{T \rightarrow \infty} \beta_T^* \neq -\alpha^*$ . Then, as  $(\beta_T^*)_{T \geq 1}$  is contained in the compact interval  $[-2/\bar{Z}, 0]$  with  $\lim_{T \rightarrow \infty} \beta_T^* \notin \{-2/\bar{Z}, -\alpha^*, 0\}$ , we extract a convergent subsequence  $(\beta_{T_k}^*)_{k \geq 1}$  with limit

$$\bar{\beta} := \lim_{k \rightarrow \infty} \beta_{T_k}^* \in (-2/\bar{Z}, 0) \setminus \{-\alpha^*\}.$$

Choose a compact interval

$$K \subset (-2/\bar{Z}, 0) \setminus \{-\alpha^*\}$$

such that  $\bar{\beta} \in \text{int}(K)$ . Then  $\beta_{T_k}^* \in K$  for all sufficiently large  $k$ . By Lemma E.8, it follows that  $|G'_{T_k}(\beta_{T_k}^*)| \geq c_K > 0$  for all sufficiently large  $k$ . This immediately contradicts the nature of  $(\beta_{T_k}^*)_{k \geq 1}$  as a sequence of stationary points for  $(G_{T_k})_{k \geq 1}$ . Therefore, one must have  $\bar{\beta} = -\alpha^*$  and as the subsequence  $(T_k)_{k \geq 1} \subseteq \mathbb{N}$  was arbitrary, convergence for the entire sequence  $(\beta_T^*)_{T \geq 1}$  to  $-\alpha^*$  holds:

$$\lim_{T \rightarrow \infty} \beta_T^* = -\alpha^*. \quad (\text{E.15})$$

Convergence of  $\lim_{T \rightarrow \infty} \alpha_T^* = \alpha^*$  follows from (E.15) and the identity  $\alpha_T^* = \alpha^*(\beta_T^*)$  for all  $T \geq 1$ .  $\square$

The above result concludes the proof of Theorem 6.3.

## F Ablation Experiments

In this Appendix, we examine the significance of the  $S_t$  skip-connection and the CA between the layer outputs  $(F_t)_{t \geq 0}$  and the original raw data  $X$ —displayed in Figure 1. To this end, we compare, empirically, the trained performance of the one- and two-parameter LCA models defined in Section 5 against ablated models. We introduce three new architectures in the one- and two-parameter settings. First, consider the one-parameter LCA model without  $S_t$  (equivalently with  $\alpha \equiv 0$ )—that is, we modify (5.2) to be

$$\mathbf{F}_t = \mathbf{F}_{t-1} + \mathbf{A}_{t-1}$$

and operate with one learnable parameter as in Section 5.1. Second, building off the preceding model, we now set  $\mathbf{A}_t = \mathbf{A}(\mathbf{Q}_t, \mathbf{K}_t, \mathbf{V}_t)$  with

$$\mathbf{V}_t = \alpha \mathbf{F}_t, \quad \mathbf{K}_t = \mathbf{Q}_t = \mathbf{F}_t, \quad (\text{F.1})$$

so that  $\mathbf{A}_t$  is no longer a LCA implementation, but rather is LSA applied to  $\mathbf{F}_t$  with a single learnable parameter. We refer to this architecture as a “one-parameter deep LSA without  $S_t$ ” to delineate it from the single-layer LSA model of Section 4. Lastly, as a final trainable comparison, we consider the LSA modification given in (F.1) and re-introduce  $S_t$  (again producing two learnable parameters) in the architecture, and refer to this ablation as a “two-parameter deep LSA.” As a naive baseline, we also consider the in-context sample mean:

$$\bar{y}_{L_{te}} = \frac{1}{L_{te}} \sum_{i=1}^{L_{te}} y_i.$$

In Figure 4, we see that the removal of the  $S_t$  skip-connection in the embedding architecture compromises model performance. Notably, in the simplified one-parameter setting, the ablated models fail to improve upon the naive in-context sample mean. Moreover, in Figure 5, we see that, swapping the LCA mechanism for LSA on  $F_t$  while keeping the  $S_t$  skip-connection deteriorates model-performance, albeit improving upon the sample mean baseline and the single-layer LSA model. This further emphasizes the utility of the cross-attention and particularly of our novel  $S_t$  component.

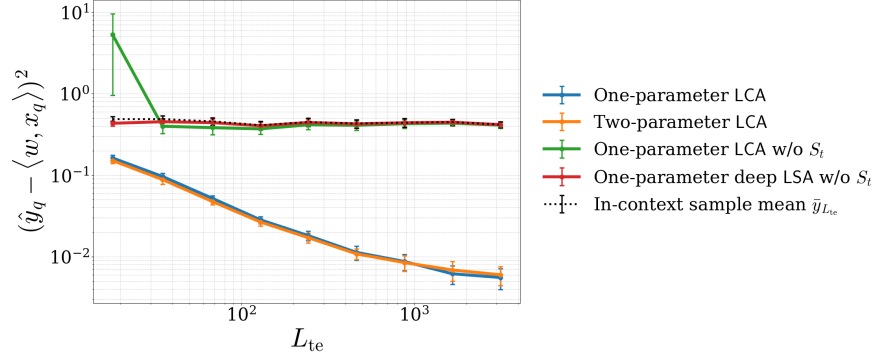


Figure 4: In-context performance at various  $L_{te}$  of one- and two-parameter LCA-based models, ablations without  $S_t$  ( $T = 10$ ), and the sample mean  $\bar{y}_{L_{te}}$ . Models are optimized on  $\ell_{N, L_{tr}}$  ( $L_{tr} = 100, N = 2000$ ) using gradient descent. Performance is averaged over 1000 test-prompts where error bars represent standard deviation over 10 separate training runs.

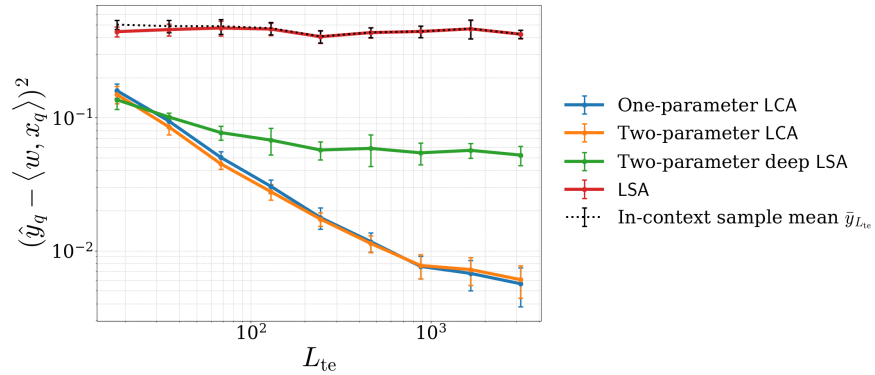


Figure 5: In-context performance at various  $L_{te}$  of one- and two-parameter LCA-based models, two-parameter, deep LSA model ( $T = 10$ ), the LSA model from (4.2), and the sample mean  $\bar{y}_{L_{te}}$ . Models are optimized on  $\ell_{N, L_{tr}}$  ( $L_{tr} = 100, N = 2000$ ) using gradient descent. Performance is averaged over 1000 test-prompts where error bars represent standard deviation over 10 separate training runs.

## G Visualization of the Loss Landscape

The rationale behind the initializations given in Theorem 6.3 and discussed in Section 6 are supported in Figure 6 which illustrates a steep valley along the curve  $\{(\alpha^*(\beta), \beta) : \beta \in (-2/(\bar{m} + 1), 0)\}$  as  $\alpha^*(\beta) \approx -\beta$  ( $\alpha^*(\beta) \rightarrow -\beta$  as  $T \rightarrow \infty$ ) in this window. To contrast our setting with a more sophisticated model, we also plot the loss landscape of the two-parameter model where pre-Layer Normalization [Xiong et al., 2020] is added between the LCA layers. Interestingly, this model reveals a similarly located and sized ravine in the loss landscape, hinting at the insights from our ablated setting to more complex models.

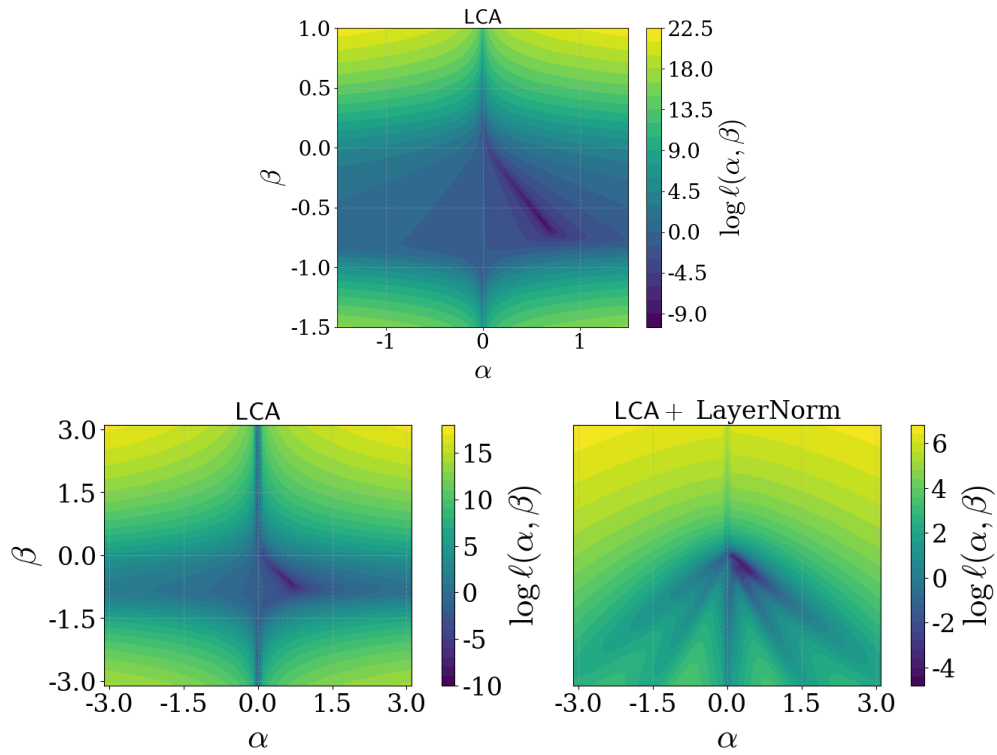


Figure 6: Log-scale heat map plots of the two-parameter loss  $\ell(\alpha, \beta)$  at depth  $T = 10$  (**top**) and  $T = 5$  (**bottom**) where  $\|\mathbf{m}\| \sim \text{Unif}(0, 2)$ . At depth  $T = 5$ , we compare the LCA-based model considered herein (**bottom left**) with the addition of pre-LayerNorm between the CA layers (**bottom right**).